NATIONAL TECHNICAL UNIVERSITY OF ATHENS

School of Naval Architecture and Marine Engineering

Excessive Acceleration Second Generation Intact Stability Criteria Compared with Cargo Securing Manual

Diploma Thesis

Ioannis Mariolis Konidaris

SUPERVISOR

Konstantinos Spyrou

Professor, Section of Ship Design and Maritime Transport, NTUA

Athens,

September 2024

Abstract

The rapid growth in global trade has led to the development of larger ships with significantly increased cargo capacity. While these advancements have improved economic efficiency worldwide, they have also introduced new challenges in ship stability and safety, particularly under heavy weather conditions. This thesis investigates the critical factors affecting ship stability, focusing on the phenomenon of excessive lateral acceleration and its impact on both the crew and cargo, with a special emphasis on container loss at sea. It examines, analyzes and compares the criteria developed by IMO concerning the lateral accelerations of a ship.

The study begins with a brief overview of the history of stability theory, from the age of Archimedes to the present day. It highlights the evolution of the most important stability concepts, like the metacentric height and the righting lever. The study also reviews the initial criteria developed by IMO, focusing on the stability of the ship, which are the General Stability Criteria and the Weather Criterion. The Second Generation Intact Stability Criteria represent a substantial upgrade over the earlier existing criteria. It contains five different vulnerability criteria, one of which is the Excessive Acceleration criterion, which is a primary focus of this diploma thesis. Additionally, the study examines another IMO-developed criterion, the Cargo Securing Manual, especially focusing on the forces developed on the container lashings due to the ship's lateral movements.

The regulatory framework of Level 1 and Level 2 of Excessive Acceleration criterion and the Cargo Securing Manual is then analyzed and explained. The study was motivated by the need to understand whether these two sets of criteria present conflicting requirements or overlaps. A code using the programming language of Wolfram Mathematica is developed, in order to perform the calculations contained in the two criteria. The calculations are conducted using a model ship for four different loading conditions. The results are then discussed, providing an insight on the relationship between the criteria. The differences and similarities of the two are noted. Various parameters are changed, to check which one affects the criteria the most. Finally, the questions of which criterion is stricter and if the application of only one of them seems sufficient, are answered.

Acknowledgements

Firstly, I would like to thank my professor and supervisor K. Spyrou for giving me the opportunity to work on such an interesting subject. I am very grateful for his advices that helped me in deeply understanding the topic and his guidance and references that were crucial in shaping this thesis. His teachings, both during his classes and throughout the development of this thesis, have been invaluable and greatly appreciated.

In addition, I would like to thank all my friends and colleagues that have been by my side for the entire duration of this academic journey. Their encouragement and emotional support have been a constant and vital source of motivation all these years. In particular, I want to express my gratitude to Aris, Ilias, Giorgos, Dimitris, Marios and Maria for always being there for me.

Finally, I have to thank my family for their continuous advices, support and understanding in every decision I made thus far. They have greatly formed the person I am today and have provided me with everything I needed to reach to this point.

Table of Contents

List of Figures

List of Tables

Chapter 1: Introduction

The gradual and continuous rise in the demand for transporting goods has pushed the naval architects to design ships much bigger in capacity and size compared to the ships a few years ago. This has achieved many great things, efficiently transferring an immense amount of cargo, lowering the travel time and overall improving the global economy. It seems important to be mentioned that, 80-90% of the supply chain worldwide is transported by ships. However, for those be accomplished, naval architects had to change the design of their ships by enlarging their size and greatly altering their main dimension ratios. This increase in demand, can pose numerous challenges, regarding the safety of the ship, its cargo and its crew.

Not a few instances have been recorded, recently where passengers of the vessel have lost their lives or have been seriously injured on board, when the ship was under heavy weather. When faced with severe waves and strong winds, the ship experiences intense lateral movements causing crew members, usually located in the bridge deck, to lose their balance, resulting in serious injuries, and sometimes even fatalities.

Moreover, the loss of cargo, especially containers, has been a growing problem. In the last decade, researches show that the annual number of containers lost is over 2000 and potentially even exceeded 10000 in some years [1]. Official reports indicate approximately six incidents of lost containers per year, but the actual number is likely significantly higher. The containers lost can be very harmful for the environment, when containing dangerous substances like explosives or toxic chemicals. The content of the fallen over containers, however, can often be unknown, posing a problem of uncertainty, regarding whether immediate salvage actions should be initiated or not.

Many reasons can be analyzed explaining these incidents. Nonetheless, the common factor among all of them, is the excessive acceleration generated in the roll direction, coupled with significant roll angles. Some specific loading conditions, close to ballast, can lower the center of gravity and result in large metacentric height. This, combined with adverse weather conditions, sometimes causes the ship to attain large angular velocity laterally, endangering the well-being of both the crew and the cargo. The forces applied on the lashings of the containers on the main deck are greatly amplified the further they are located from the midpoint, even exceeding their yield strength. Consequently, they are at greater risk of falling into the ocean or at the main deck, tipping over nearby containers.

Another contributing factor for the loss of containers can arise from careless stacking and securing practices. There are rules regarding the stowage of the containers, that must be followed, which are sometimes neglected. According to these rules, heavier containers are supposed to be stored in lower tiers and lighter ones higher, in order to avoid any stability issues. However, the lack of knowledge of the exact content of each container, creates an ambiguity of where each container has to be stored. Additionally, the absence of a precise definition for heavy and light container, magnifies the issue.

Inadequate strength of the lashings and their improper placement are two additional reasons contributing to the loss of cargo. Ship movements can cause slight shifts of the containers,

which further stretches the securing cables, intensifying the acting forces. The wide array of securing systems creates confusion and complicates the resolution of the problem. Overstacking the containers on the upper deck, creates both a visibility problem for the Master from the bridge and greatly reduces freeboard. The lack of visibility decreases the ability of the captain to react in time avoiding upcoming waves and obstacles and generally hazardous situations. The lowering of the freeboard causes the deck to immerge in a very small roll angle, making the capsizing of the ship way more probable.

To avoid all those incidents and mitigate these problems, IMO and flag state had to develop a set of rules and regulations. In 1998, SOLAS updated the Chapter VI – Carriage of Cargoes, in order to contain the Cargo Securing Manual (CSM). This Manual contains all the important information for the Master, including but not limited to, information about stowage and securing of the cargo units, types of securing devices aboard ship, the maximum loads of the lashings and the calculations for determining the forces applied to them. The calculations have to be made for every loading condition. Given the lack of specific data, regarding the sea conditions and the ship response to waves the calculations are approximate and based on the dimensions of the ship and the size of the containers. All the containers aboard the ship have to be stowed and secured according to the CSM, throughout the whole duration of the voyage.

Additionally, in 2020, IMO introduced the Second Generation Intact Stability Criteria (SGISC). These criteria include five new dynamic stability failures. IMO provides specific guidelines in order to determine if a ship, in a specific loading condition, is vulnerable to each stability failure. A ship has to be classified as non-vulnerable to all five instabilities and for all loading conditions, in order to be safe to travel. One of the five instability cases is Excessive Acceleration (EA). This criterion ensures that the lateral acceleration of the ship will not become too high, putting at risk the crew to lose their balance and injure themselves. In subsequent chapters of this diploma thesis, the calculations for both the CSM and the Excessive Acceleration criterion will be conducted and the results for a sample ship will be presented and analyzed.

Chapter 2: Critical Review and Thesis Objective

2.1 Historical Review

2.1.1 Stability Theory [2]

The concept of ship stability has been known from ancient years. The first notable mention about ship stability theory was made by Archimedes around 250 BC. Alongside his research regarding the buoyancy of submerged objects (Archimedes Principle), he conducted experiments with paraboloids in order to calculate their resting positions in liquid's surface. His studies included scenarios where the body's base was completely out of the liquid as well as when it was partially or fully submerged. Many years later, his work inspired multiple scientists, including Galileo, who studied the resting points of conical shapes.

For almost two thousand years the matter of ship stability was not widely discussed. During the Age of Enlightenment, however, it suddenly resurfaced and was a pressing issue, concerning researchers and scientists from all over Europe. They recognized the significance of a ship's center of gravity in determining its stability. Multiple individuals conducted experiments, in order to estimate it. In 1697, French priest and mathematics professor Paul Hoste, placed weights at the top of ships' mast and measured its roll angle. Subsequent experiments, by shipbuilders Juan Santacilia in 1771 and Fredrik Chapman in 1775, involved shifting the position of weights on the deck and observed the response of the ship. At the time, the analytical calculation for the center of gravity appeared too difficult and time-consuming.

In 1749, Euler's *"Scientia Navalis"* (Naval Science) looked into the concept of equilibrium and laid the theoretical framework for modern day hydrostatics. He understood that for a submerged object to be in equilibrium, the gravity force and the buoyancy have to be equal and applied in the same line with opposite directions. He pondered what would happen if a small disturbance changed that, and the two forces where no longer collinear. He figured out a criterion to characterize if an object is in a stable, unstable or neutral equilibrium state. He realized that for a ship to be stable the presence of righting moment is required. He then calculated the righting moment for small roll angles with the use of the immerging and submerging wedges.

Arguably, the most significant work of that period was the book of the French mathematician Pierre Bouguer *"Traité Du Navire, de sa construction, et de ses mouvemens"* (Treatise on the ship, its construction and its movements). Almost simultaneously with Euler, in 1746, Bouguer published his book on the subject of ship stability. He was one of the first people to explore the concept of metacentric stability. He gave the definition of metacenter as the point of intersection between the buoyancy force line and the vertical line passing through the center of gravity. He proposed using the metacentric height (GM), meaning the distance between the metacenter and the center of gravity, as a measure of stability. He also came up with the formula for the length of the metacentric radius (BM), meaning the distance between the center of buoyancy and the metacenter, based on the ship's dimensions. It defined it as the fraction of the second moment of the waterplane area around the longitudinal axis, over the volume of displacement:

$$BM = \frac{I_T}{\nabla}$$

In his work, Bouguer also gave the formula for the metacentric height GM:

$$GM = BM + KB - KG$$

Where KG is the height of the center of gravity and KB is the height of the center of buoyancy. For all of these formulas, methods or experiments have been made, to calculate them. Therefore, he made clear that you can compute the GM, only by knowing the ship's hull form and the position of the center of gravity. He realized that if the GM is known, the righting lever (GZ) for all small roll angles (φ) is easily computed as:

$$GZ = GM \cdot \sin\varphi$$

So, for every small angle φ, the righting lever can be calculated, and so can the righting moment (righting lever multiplied by the buoyancy), meaning the ability of the ship to return to its initial stable position or its stability. Euler's and Bouguer's books were two very important breakthroughs in world of naval engineering, with many applications in today's practices.

The problem with Bouguer's theorem is that the metacenter in not a fixed point as the ship develops bigger roll angles. The estimation that it remains stationary, gives satisfying results only in small angles. Thus, the new challenge for researchers was to find a way to compute the GZ for every angle, without using a stationary metacenter. Notable efforts were made by Atwood in his reports, in 1796 and in 1798, where he gave a formula for GZ using the submerging and emerging wedges. Barnes, in 1861, gave a more precise and practical method of Atwood's work, using the Simpson's theorem. In 1867, the work of John for the British Navy, established the righting lever curve GZ-φ, as the main measure of stability, which is still in use in stability criteria today.

2.1.2 History of Intact Stability Criteria

General Stability Criteria

As previously stated, the righting lever GZ was the main factor characterizing a ship as stable or not from the 18th century. However, it wasn't until 1913, when Benjamin established the first formal stability criteria, using the dynamic stability lever. He defined specific limits for its values at roll angles of 30 and 60 degrees. Despite his efforts, Benjamin's criteria failed to gain wide acceptance of the public.

In 1935, Pierrottet introduced new criteria, who followed a similar approach as Benjamin. He also utilized the dynamic righting lever and required for it to be sufficiently large to overcome the ship's deviation from its equilibrium position, caused by waves, wind and the movement of people onboard. Th criteria seemed too strict for the ship designs of the time.

In 1939, Rahola proposed a series of conditions for the righting lever curve, GZ-φ as a part of his PhD thesis. He was trying to figure out the standards for a ship (minimum metacentric height GM and righting arm GZ), to be sufficiently characterized as stable or not. He pointed out that the method to calculate the vessel's stability was more than 200 years old (Bouguer's work), so specific standards showing the minimum stability of a ship should have already been created [3].

Rahola's conditions were later used by IMCO (later named IMO), in 1969, to create the *general stability criteria*, who are still in effect today. These criteria were only recommendations for cargo and passenger ships under 100 meters in length [4]. In 2008, these criteria got revised and updated and for all ship designs after 2010 became the following: [5]

1. The area under the GZ curve between 0 degrees and 30 degrees (area A1 as shown in Figure 1) has to be more than 0.055 meter-radians
2. The area under the GZ curve between 0 degrees and 40 degrees (area A1 and A2 as shown in Figure 1) has to be more than 0.09 meter-radians
3. The area under the GZ curve between 30 degrees and 40 degrees or between 30 degrees and the down-flooding angle φ_f, if φ_f is less than 40 degrees (area A2 as shown in Figure 1) has to be more than 0.03 meter-radians
4. GZ has to be at least 0.2 m for a roll angle equal or more than 30 degrees
5. The maximum value for GZ has to occur at an angle of 25 degrees or more and if practicable at an angle greater than 30 degrees
6. Initial metacentric height GM_0 has to be more than 0.15m

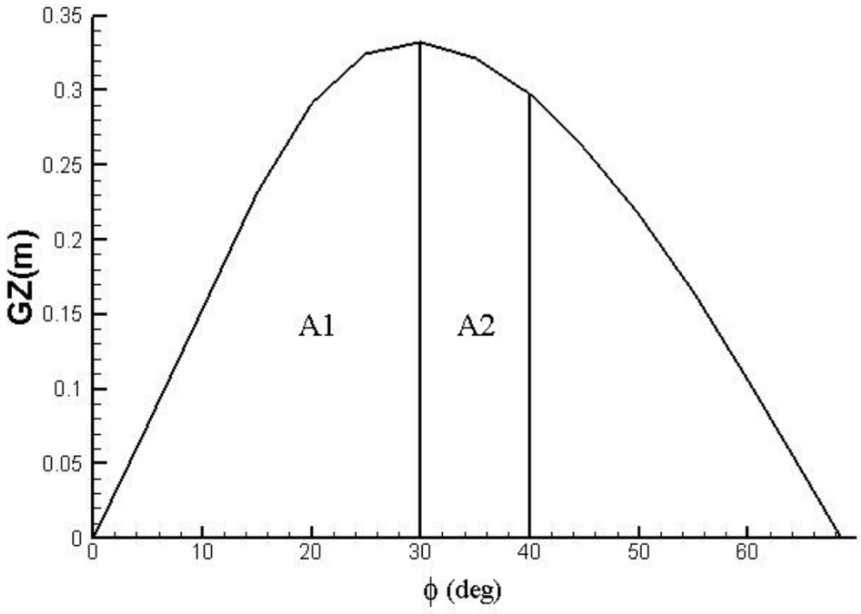

Figure 1: GZ Curve [6]

Weather Criterion

The problem with Rahola's standards, and later IMCO's regulations , is that they didn't take into account the response of the ship under heavy waves and strong winds. That pushed IMO, in November of 1985, to recommend the *weather criterion*, for all passenger and cargo ships over the length of 24 meters and for all fishing vessels over the length of 45 meters [7]. This suggestion constituted the first dynamic standard and ensured that the vessel could withstand heavy weather condition, even with the main engines down, losing the ability propel itself, or in *dead ship condition.* Its physical background was widely based on the work of the Japanese researchers Yamagata (1959) and Watanabe (1938), combined with the Russian standards (1961), like the work of Blagoveschensky [2, 8]. The criterion was already enforced in other countries including Japan, Australia and in the US Navy [3]. In 1993, IMO adopted the Intact Stability code (IS code), which was a combination of the *general stability criteria* of 1969 and the *weather criterion* of 1985 [9]. Both of these criteria were revised and updated, as previously stated, in 2008 [5].

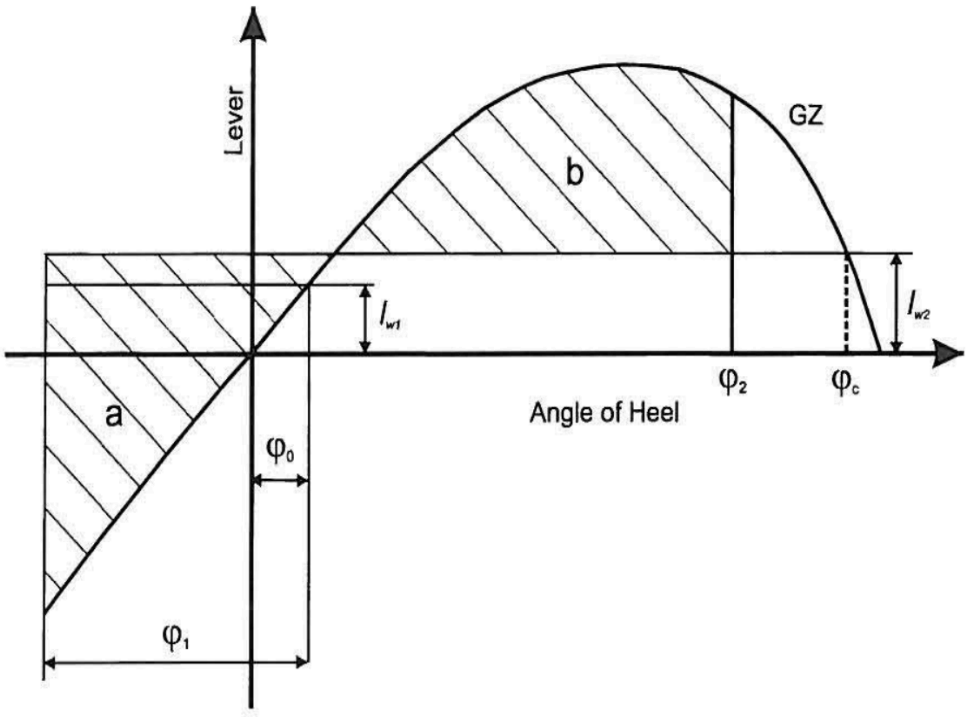

Figure 2: Weather Criterion [5]

The criterion computes the righting and the heeling moment and requires the first to be larger than the second, in order to withstand the rolling, due to winds and waves, and in other words be regarded as stable. It's assumed, that the ship is under a steady wind pressure with heeling lever l_{w1}. Due to the wind force, the ship is in equilibrium in the angle φ_0, from where it rolls

windwards, under the action of waves, until the maximum heeling angle φ_1. It then gets subjected to a wind gust, with a heeling arm l_{w2}. The angle φ_2 is the smallest of φ_f, φ_c and 50 degrees. The angle φ_f is called angle of down-flooding and is the angle where non watertight opening of the main hull or of the superstructures begin to submerge. The angle φ_c is the second interception between the heeling arm l_{w2} and the GZ curve. For the ship to be characterized as stable and be able to return to its equilibrium position, without the probability of being capsized, the area b has to be bigger than area a, as shown in Figure 2 [5].

Second Generation Criteria

The IS code of 2008 [9] mentions some stability failures, which not all of them are covered by the criteria, but ships should still be aware of. More specifically, it mentions:

- Righting lever variations between the waves' crest and trough can cause parametric and pure loss of stability
- Vessels in dead ship condition are in danger of resonant roll
- Maneuvering challenges can occur in following waves, leading to issues like broaching and despite the Master's efforts, maintaining a steady course may prove unlikely.

From 2008, the Sub-Committee on Stability and Load Lines and on Fishing Vessels Safety (SLF) of IMO was established, in order to address the above phenomena and establish new criteria addressing them [10]. Due to their complexity, they required more time than expected to be finalized [10]. After almost more than 10 years, in 2020, IMO established them and were named the *Second Generation Intact Stability Criteria* (SGISC). As of now, they are the most scientifically advanced criteria, on the set of regulations of IMO [2]. They did not replace IS code and the general stability criteria, and are not mandatory and are still under review. However, IMO recommended that the shipping community apply them, so that sufficient data can be collected and so they can be tested and later revised [11].

The SGISC are mentioning five different stability failures, which all of them have to be tested by the ship. The five types of failure modes are the following:

- Dead ship condition
- Excessive acceleration
- Pure loss of stability
- Parametric roll
- Surf – riding / broaching – to

Dead ship condition failure mode is an update of the weather criterion of 2008. It checks the ability of the ship to stay afloat, even with the main engines down, having no means of propulsion and the simultaneous act of wind and waves.

Excessive acceleration appears in ships with high GM value, usually close to the ballast condition. Large lateral acceleration values can put the crew and the cargo of the vessel in danger. Due to the angular velocity being constant, along the heights of the ship, higher positions from the roll axis experience greater lateral acceleration, as they cover more distance

in the same time frame [10]. Therefore, this puts people in higher places, such as the bridge deck, in bigger danger to lose their balance and injure themselves.

Pure loss of stability is a phenomenon that appears when the ship and a following wave have very similar speeds. When the ship is at the crest of such a wave, the righting arm obtains very small values and even negative ones. When that happens, the ship tends to diverge from the upright position and gain a big rolling angle. The ship can even capsize, if it stays long at the wave crest [2].

Parametric roll appears in the presence of heading or following waves, with wavelengths similar as the length of the ship, when the ship is at their crest or at their trough. When the middle of the ship is at the top of the crest, the surface area of its waterplane is greatly reduced and oppositely increased when in trough. This periodical change of waterplane area affects the righting arm which follows a similar periodical form. This constant oscillation of the GZ, triggers a dynamic movement which can result in an intense rolling motion with big heeling angles, even with small disturbance, when otherwise would seem harmless [2].

Finally, broaching – to occurs, again in following high waves and usually in vessels with smaller length. When the ships are at the top of the wave, heading downwards, the phenomenon surf – riding can happen. During that phenomenon the wave pushes the ship forward, forcing it to increase its speed and causing it to turn towards the wave, acquiring a heeling angle and getting endangered to overturn. Broaching – to can occur after surf – riding, but can also occur when it's absent, if the ship is operating in low speeds, making the ship to lose control of the rudder and become unstable [2]. This constitutes a very complex dynamic phenomenon, which cannot be analyzed further in the current diploma thesis.

The SGISC employ a multilayered approach, with three levels of assessment. Each level progressively offers greater accuracy and complexity than the preceding one. If one level proves that the ship is not vulnerable, there is no need to proceed to the next one. If all three levels give negative results, then some operational measures are suggested in the guidelines [11]. A graphic depiction of that process, can be seen in Figure 3. Level 1 is constituted by straightforward calculations, utilizing estimation formulas. It provides a rough assessment, whether the ship can be susceptible in the specific failure mode.

Level 2 of the criteria, as stated before, are more complex than those of Level 1. They employ probabilistic methods in order to calculate the probability of the ship to be considered as vulnerable to each failure type. The criteria take into account various wave conditions, depending on the wave's height and period. IMO provides a wave scatter table, created by IACS, with the likelihood of a wave with specific values for these two characteristics, to appear. Every pair of wave height and period makes up a short – term condition. For each condition a short – term failure index is computed and combining all these indices, the long – term failure index is made up. That number indicates if the ship can be considered safe from each failure type or not. Despite the amount of calculations of this level, they can be computed quickly, even aboard of the vessel.

Level 3 of the criteria is Direct Stability Assessment (DSA). DSA predicts as reliably as possible the exact movements of the ship, when is afloat, providing an exact answer of whether

the ship is susceptible to a type of failure [10]. However, DSA is a complex and time consuming procedure, requiring the latest technological advancements, such as Computational Fluid Dynamics (CFD) and detailed mathematical models. It can also be done with experimental methods, if it provides the same amount of accuracy, but can be proven very expensive. IMO guidelines suggest a few numerical methods the ship owner can follow, to conduct the DSA [11]. It can often prove more advantageous for the ship owner to skip the DSA and go straight to altering the ship's operating conditions. That way the ship can still be able to pass Level 1 or Level 2 criteria and save the time and money, DSA requires. DSA was intended as a tool for special cases, for example with a new type vessel with modern design, and not to be used regularly [12].

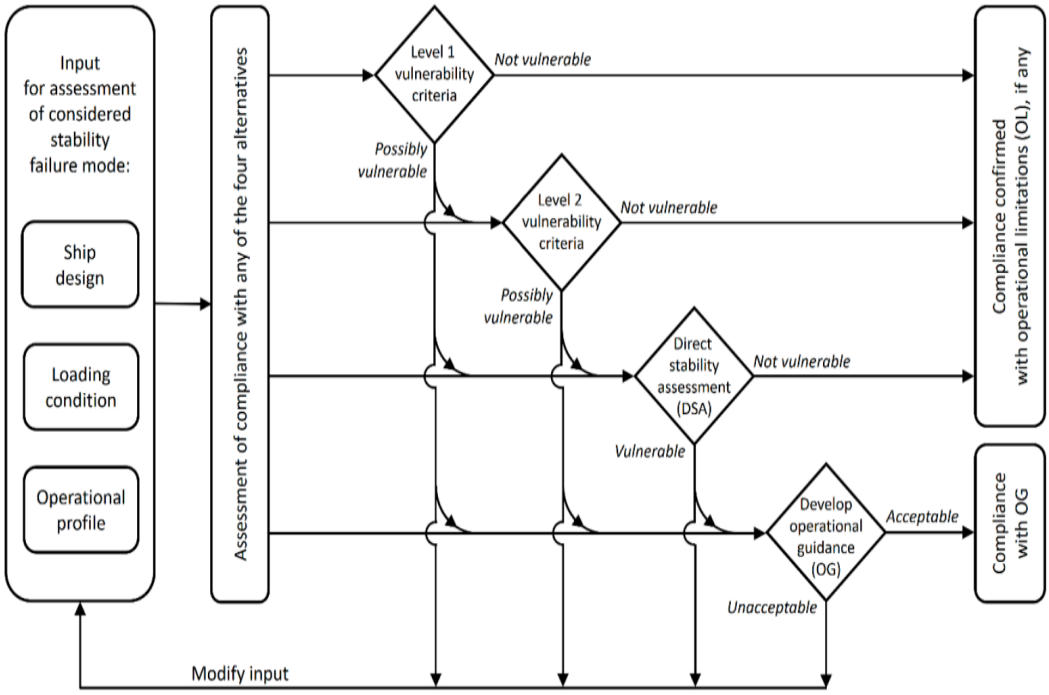

Figure 3: Simplified scheme for the application of SGISC [11]

2.1.3 Accidents due to Excessive Acceleration

As previously stated, Excessive Acceleration was not mentioned in 2008's IS code, as a possible failure type. However, two specific accidents that happened in 2008 and 2009 forced IMO to include it in their research for the Second Generation Criteria. Both accidents included casualties, because of intense lateral accelerations, that were developed in the area of the bridge of the ship. The two ships were named Chicago Express and CCNI Guayas. More specifics about these accidents are analyzed below. All the data presented below are collected by the Federal Bureau of Maritime Casualty Investigation (BSU) from their investigation reports 510/08 [13] and 391/09 [14] for the Chicago Express and the CCNI Guayas, respectively.

Chicago Express [13]

Chicago Express was a German containership, shown in Figure 4, with the characteristics shown in Table 1. In November of 2008, it was sailing away from the port of Hong Kong, towards the port of Ningbo in China. The typhoon "Hagupit" was approaching and the Master received instructions from the port authorities, to pay caution. In the late hours of the day, the ship came across heavy winds, causing the vessel to develop rolling angles as big as 32 degrees. The Master tried to escape the weather, by deviating from the pre-decided course, heading to Ningbo, reducing the roll angles to 20 angles. Shortly after midnight of the next day, Chicago Express was hit by a strong wave, which caused it to roll several times around its axis. A maximum of 44 degrees of heeling angle was recorded, with a period of around 10 seconds. This created huge accelerations in the bridge deck, causing the three out of four people there, to lose their balance and fall to the ground. The fourth crew member, the Officer on Watch, managed to hold onto something, to keep his balance and ran to check on everyone else. One of the fallen over crew members was uninjured, but the other two, the Captain and an AB (Able Seaman), laid unconscious. After first aid, they the Captain managed to regain his conscious and later, when the weather calmed, he was transported to the hospital, via helicopter. Unfortunately, they couldn't save the passed out AB, who after around two hours lost his life, due to head injuries. The Captain, despite his serious internal injuries, threatening his life, managed to get healed and recovered significantly.

The main cause of the accident, except from the heavy weather conditions, was the huge initial metacentric height, GM. Data show that the vessel sailed with a GM of 7.72 m, which offers sufficient stability, but results in quick return to the initial position, coupled with enormous lateral speeds. In order to, lower that value and maybe avoid the accident, the crew should have filled some of ballast tanks. However, given the fact that the ship was rushed out of the port, because of the storm, this would probably have been impossible. Apart from the two serious injuries mentioned above, four more crew members suffered from bruises and other minor injuries. 6 containers were lost in sea, but they didn't cause any serious environmental pollution. Finally, the hull of the ship was not damaged, despite the extreme weather condition it faced.

Figure 4: Photo of the Chicago Express [13]

Table 1: Main Particulars of the Chicago Express [13]

Name of the vessel:	CHICAGO EXPRESS
Type of vessel:	Container vessel
Nationality/flag:	Germany
Port of registry:	Hamburg
Vessel operator:	Hapag-Lloyd AG
Year built (keel laying/completion)	2005/2006
Classification society:	Germanischer Lloyd
Length overall:	336.19 m
Breadth overall:	42.80 m
Gross tonnage:	93811
Deadweight:	103691 t
Draught (max.):	14.61 m
Engine rating:	68640 kW
Main engine (type/manufacturer):	Diesel 12 K 98 ME Hyundai MAN
Speed (max.):	25.2 kn
Number of crew:	35 (including 8 cadets)

CCNI Guayas [14]

The second accident happened to the containership CCNI Guayas, in September of 2009, shown in Figure 5, with its particulars in Table 2. A lot of similarities can be found between this accident and the accident of Chicago Express. Both container vessels were sailing under the German flag, away from the Hong Kong port and left anchorage, because of an approaching storm. In this case, the typhoon was named “Koppu”. During the time of the accident, two people were on the bridge deck, the Captain and the Third Officer. Due to the heavy weather, the vessel was facing strong winds, reaching the speed of 10 in the Beaufort scale and waves, up to 8 meters on height. The ship started to roll intensely, reaching 35 degrees angle with about 10 seconds period, according to crew witnesses. Obviously, large lateral accelerations were developed in the highest parts of the ship. This caused, the Third Officer to slip and fall, seriously injuring himself. Despite the efforts made by the Captain and an AB, providing medication and first aid, he lost his life after a few hours. Additionally, the hull of the ship sustained some damage as a result of the strong waves.

Investigations show that the vessel was undermanned, with only 11 crew members, whereas the minimum required was 16. Moreover, 3 people were supposed to be in the bridge during the accident, but the AB was ordered to leave, due to inappropriate footwear. As the vessel began to gain accelerating rolling velocity, papers and other various objects started flying around, littering the floor and making it more slippery. No successful efforts, were made to clean it up, making the scene even more dangerous. Consequently, human error was also cited as a contributing factor of the accident in the investigation report.

Figure 5: Photo of the CCNI Guayas [14]

Table 2:Main Particulars of the CCNI Guayas [14]

Name of vessel:	CCNI GUAYAS, ex Alianca Hong Kong, ex Helvetia, ex Charlotta
Type of vessel:	Container vessel
Nationality/flag:	Germany
Port of registry:	Hamburg
Year built:	1997
Classification society:	Germanischer Lloyd
Length overall:	208.16 m
Breadth overall:	30.04 m
Gross tonnage:	25608
Deadweight:	34014 t
Draught (max.):	11.40 m
Engine rating:	19810 kW
Main engine:	MAN B&W 7L 70 MC MK6
(Service) Speed:	21.5 kts
Manning:	11

The ship was sailing with no containers on board and only ballast water in the tanks. This made the center gravity significantly lower than usual, causing the GM to gain elevated values. Specifically, while departing the port the initial GM was around 6 meters, making it very stable, but also assisting in the development of great rolling accelerations, similarly to the Chicago Express. Putting less ballast water in the tanks, might have helped the situation, given that the vessel was stable enough and added ballast water, didn't contribute to that, significantly.

FRISIA LISSABON [14]

Lastly, another incident with similar characteristics, should be mentioned, in order to prove that these types of accidents are not only limited to the area nearby Hong Kong. This specific incident occurred at the North Sea, in September of 2009, with the containership FRISIA LISSABON (Figure 6), which was almost identical in characteristics as the CCNI Guayas. The vessel was heading to Rotterdam, from Emden. When the ship was at open sea, located near the Borkum island, it faced bad weather, with strong winds and big waves. Two individual large waves hit it, causing it roll heavily and making the Pilot to fall over and gravely injuring himself. Thanks to, great sea keeping and decision making by the crew, lowering significantly the ship speed and changing the course, the rolling motion quickly decreased. Fortunately, this accident didn't cause any casualties, however, the pilot hadn't been able to work again, due to his injuries, as of 2011, when the investigation report was published.

Figure 6: Photo of FRISIA LISSABON [14]

2.2 Cargo Securing Manual

The accidental discharge of containers overboard, not only results in damage or loss of goods but also puts the vessel and the crew at significant risk. Improper stacking of containers can lead to serious injuries or even fatalities during the loading and unloading operations. The shifting of containers due to roll and pitch motions, during heavy weather, impacts the stability of the ship and can ultimately lead to its capsizing. Also, depending on the content of the containers, their loss can cause environmental pollution, if hazardous materials are involved. Finally, floating containers at sea pose a navigational hazard to other nearby vessels.

During the 1980s and 1990s the number of incidents involving the loss of the containers at sea was increased significantly [1]. This prompted IMO to develop a set of rules to ensure the

safety of cargo on both open and closed decks, and to mitigate the risks previously mentioned. This set of rules was the Cargo Securing Manual (CSM). IMO (then named IMCO) firstly introduced CSM in 1981, where it included guidelines for the security and stowage of cargo units aboard ships other than cellular containerships. The CSM provided details on the location of securing arrangements and gear, instructions for the correct application of the securing devices and the accelerations and forces to be expected in various positions on the ship [15]. In 1985, IMO encouraged governments to provide with specific guidelines for the safe stowage of cargo and offered more specific instructions about the contents of the CSM [16]. The guidelines for preparing the CSM were updated in 1996 and have remained largely unchanged to this day. CSM had to be approved by the ship flag state administration and be carried aboard the ship for the entire duration of the voyage. The updated CSM, in addition to the details and location of the securing arrangements, now contains necessary information for the inspection and maintenance of the securing supplies and includes provisions for the proper training of the crew [17].

In November of 1991, IMO also issued the Code of safe practice for Cargo Stowage and Securing (CSS code), which provides recommendations for the proper stowage and securing of cargo and offers specific instructions for special shipments, such as portable tanks, rolling containers, and anchor chains [18]. The information contained in the CSS code serves as the primary guidance for the preparation of the CSM. The main difference between the CSS code and the CSM is that the first contains general information applicable to all ships, while the latter is created and applied for one specific ship and has to be carried aboard during the voyage.

The Classifications Societies also play an important role in the development and implementation of the CSM. Classification Societies with their technical expertise help in the development for the CSM. More specifically, they provide guidelines for the calculation of the expected forces and accelerations acting on cargo units aboard the vessel and the Maximum Securing Loads (MSL) of the securing arrangements [19]. Also, they are responsible to validate and approve of the methods described in the CSM and confirm that the manual of every individual ship is certified.

2.3 Thesis Objective

In the current diploma thesis, the application of the Guidelines for the Excessive Acceleration (EA) failure type of the SGISC of IMO will be conducted. More specifically, they will be implemented for Level 1 and Level 2, as DSA is deemed overly complex. The EA criterion will be applied and tested, in order to evaluate how easy and practical is to pass each Level. For each step of the Guidelines the physical background will be explained. The study will investigate whether existing vessels can easily meet the criterion, suggesting it is too lenient, or if the criterion is too strict, making it almost impossible for vessels to be considered as non-vulnerable. Various different parameters will be altered, in order to evaluate their sensitivity, their impact on the final result and their influence in whether the ship is stable or not.

Additionally, the criterion will be tested to find out if any inconsistencies occur. Inconsistencies occur when a lower Level finds the ship not vulnerable, but a next, more complicated and precise Level says otherwise. In the current thesis, the check will be whether a vessel passes

the Level 1 criterion but fails to do so for the Level 2. Consistency problems are supposedly fixed by IMO, during the development of the criteria, but some of them might still remain [10].

Finally, as previously mentioned, lateral accelerations, besides serious human injuries, can cause damage to the cargo. Particularly, for containerships, roll movements can cause containers to start shifting and moving from their original position. Such movements can exert increased strain on the securing lashings, potentially leading to their breakage and making the whole stack of containers collapse. To mitigate these risks, all containerships have to follow the regulations outlined in the Cargo Securing Manual (CSM). The CSM contains calculations for the breakage point of the lashings, taking into account the lateral acceleration.

This means that containerships have to follow two different set of rules, regarding their lateral movement. In this thesis, the calculations contained in the CSM will be conducted to examine their applicability. Furthermore, the EA criterion and the CSM will be compared, to determine their relative strictness, identify potential overlaps, and assess whether the implementation of one criterion can be deemed unnecessary, if the vessel is considered not vulnerable according to the other criterion.

Chapter 3: Explanation of Regulatory Framework

3.1 Excessive Acceleration Criteria

Large roll angles and immense lateral accelerations pose a safety risk to crew members aboard the vessel. People at the bridge of the ship and other areas that they may be present, can lose their balance and seriously damage themselves. The Excessive Acceleration (EA) Criteria ensures that in no place of the vessel will accelerations higher than a predefined threshold will occur. The regulation applies to places of the vessel that passengers or crew will normally be present when on duty and during bad weather. Other places, like the Compass Deck, which are only accessible by vertical stairs and passengers would not usually be present during a storm, are not considered. Although the calculations can be applied to all the lengths and heights along the ship, it makes sense to check only the worst-case scenario, meaning the location where the horizontal acceleration due to the roll motion is the highest, which is the Bridge Deck (being the farthest from the roll axis). Thus, all the calculations for the EA in this diploma thesis are made at this point.

According to IMO Guidelines [10], for a ship to be able to develop excessive lateral acceleration, two specific conditions related to the vessel's characteristics have to be met for each loading condition. Therefore, the regulations described below, for both Levels, are only applicable to ships for which the following conditions are true:

$$h_w > 0.7 \cdot B$$

$$GM > 0.08 \cdot B$$

Where, h_w is the distance from the waterline to the highest point of the ship that crew or passengers may be present (meaning the bridge deck as explained earlier) and B is the breadth of the ship.

The method analyzed below, for Level 1 and Level 2 criteria are according to IMO's Interim Guidelines [11], except when cited otherwise.

3.1.1 Level 1 Framework

As previously stated, Level 1 of the Interim Guidelines is an initial calculation for the lateral accelerations. If the ship is found not vulnerable, no further calculations should be conducted. Otherwise, Level 2 assessment should be conducted and if the ship is still found vulnerable in a particular loading condition, Direct Stability Assessment (DSA) should be applied. Level 1 utilizes mathematical formulas, in order to estimate the value of the roll angle and the lateral acceleration. The acceleration in every location where crew or passengers may be present, should below a specific threshold, around half a g (4.64 m/s^2).

The formulas used in the Level 1 criterion are either based on the definition of the quantities with some made assumptions, or empirical formulas. More specifically, to calculate the roll

acceleration, the basics of ship dynamics are utilized and the values for the characteristic roll angle and the natural roll period are needed. The characteristic roll amplitude is estimated using the wave steepness (given as a function of the natural roll period), the wave steepness coefficient (estimated based on the ship dimensions and the natural roll period), and the decrement of roll decay.

The process is described in detail below:

Criterion Formula

In order for the ship, to be classified as not vulnerable in respect of the Level 1 Excessive Acceleration failure mode the following should be true:

$$\varphi \cdot k_L \cdot (g + 4\pi^2 h_r / T_r^2) \leq R_{EA1}$$

Where:

- φ: the characteristic roll amplitude (rad)
- k_L: factor taking into account the simultaneous actions of roll, yaw and pitch motions8
- $g = 9.81$ m/s^2: the gravitational acceleration
- h_r: height above the roll axis where crew or passengers may be present (m)
- T_r: the natural roll period (s)
- $R_{EA1} = 4.64$ m/s^2

The left side of the inequality represents the lateral acceleration of the ship in a specific loading condition and place of the ship where crew or passengers may be present. The right member of the inequality is a predefined value, acting as a threshold which the acceleration should not exceed, in order for the ship to not be considered vulnerable. The value was selected in a way so that the crew would not be in danger of damaging themselves during the lateral movements of the ship, while also ensuring consistency between Level 1 and Level 2 criteria.

Equation Explanation

As shown in the Figure 7 the ship rotates around a roll axis (point R). The height of the roll axis in this diploma thesis is considered fixed and assumed to be in the midpoint between the waterline and the vertical center of gravity of the vessel (point G). A random point on the ship experiences the vertical acceleration a_v due to the pitch and heave motions, the horizontal acceleration a_h due to the yaw movement and the lateral acceleration a_φ due to roll, which is vertical to the line connecting the random point and the roll axis of the ship [20].

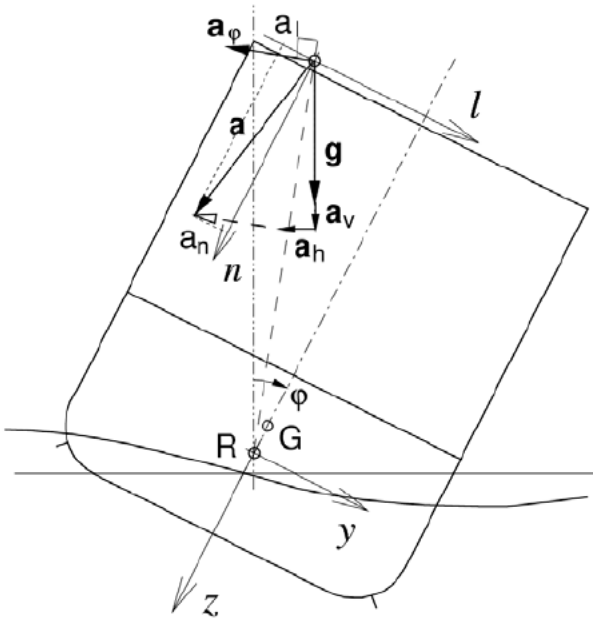

Figure 7: Accelerations at a point in a rolling ship [20]

The acceleration a_φ consists of an acceleration proportional to the roll acceleration $\ddot{\varphi}$ and two accelerations caused by the Coriolis and centrifugal forces. The latter two are neglected. For harmonic waves and therefore harmonic roll movement the roll angle is:

$$\varphi = \varphi_a \cdot \sin\omega t$$

Where φ_α is the roll amplitude and ω the roll frequency. So, the roll acceleration is:

$$\ddot{\varphi} = -\varphi_a \cdot \omega^2 \cdot \sin\omega t = -\omega^2 \cdot \varphi$$

And the a_φ acceleration:

$$a_\varphi = -\omega^2 \cdot \varphi \cdot h_r$$

Where h_r as mentioned above, is the distance of the point of interest from the roll axis. So, the total lateral acceleration (in the y-axis) will be:

$$\alpha_y = (g + a_v) \cdot \sin\varphi + \omega^2 \cdot \varphi \cdot h_r$$

For small angles (where $\sin\varphi=\varphi$) it can be rewritten as:

$$a_y = (g + a_v + \omega^2 \cdot h_r) \cdot \varphi$$

The wave frequency is taken equal to the natural roll frequency:

$$\omega = \frac{2\pi}{T_r}$$

Where T_r is the natural roll period. The a_v can be expressed as an additive factor k_L. For $\varphi=\varphi_\alpha$ the formula gives the maximum value for α_y which is what will be compared to the threshold R_{EA1}. So, a_y is rewritten as:

$$a_y = (g + (2\pi/T_r)^2 \cdot h_r) \cdot \varphi_\alpha \cdot k_L$$

Which is the formula given in the criterion. The criterion neglects the effect of the heave motion alone and takes into account only the pitch and yaw motion. Those two movements depend on the longitudinal position on the vessel, so the closer at the midship of the vessel the smaller their effect is. The formula for the k_L factor is:

$$k_L = 1.125 - 0.625 \cdot \frac{x}{L_{BP}} \ , \qquad \text{if } x < 0.2 \cdot L_{BP}$$
$$k_L = 1 \ , \qquad \text{if } 0.2 \cdot L_{BP} < x < 0.65 \cdot L_{BP}$$
$$k_L = 0.527 + 0.727 \cdot \frac{x}{L_{BP}} \ , \qquad \text{if } x > 0.65 \cdot L_{BP}$$

Where x is the longitudinal distance where crew or passengers may be present from the aft end of the ship and L_{BP} is the ship length between perpendiculars. The natural roll period Tr, is estimated by the following formula, due to the lack of adequate data for its precise calculation or measurement:

$$T_r = \frac{2 \cdot C \cdot B}{\sqrt{GM}} \text{, where } C = 0.373 + 0.023 \cdot (B/T) - 0.043 \cdot (L_{WL}/100)$$

Where B is the moulded breadth of the ship, T is the mean draft, L_{WL} is the length of the ship at the waterline and GM is the metacentric height in calm water.

For the height of the roll axis h_{roll}, SGISC estimates that it is in the midpoint between the waterline and the center of gravity. Meaning:

$$h_{roll} = KG + \frac{(T - KG)}{2}$$

measured from the baseline.

Characteristic Roll Amplitude

The roll angle amplitude in the criterion is estimated using the formula:

$$\varphi = 4.43 \cdot r \cdot s / \delta_\varphi^{0.5}$$

Where:

- r: wave slope coefficient
- s: the wave steepness, expressed as a function of the natural roll period
- δφ: non-dimensional logarithmic decrement of roll decay

The wave slope coefficient r is a correction factor representing the adjustment needed for the roll excitation moment caused by waves. It depends on the roll period of the vessel so usually it's annotated as r(ω). However, for Level 1, only the coefficient for the natural roll period is needed, so it will just be written as r. For its calculation, a lot of methods and estimations have been introduced. The simplest one is an empirical formula, used in the weather criterion of 2008 [21]:

$$r = 0.70 + 0.63 \cdot \frac{OG}{T}$$

Where OG is the vertical distance between the waterline and the center of gravity or similarly:

$$OG = KG - T$$

According to experiments, the above formula shows that it underestimates the value for the wave slope coefficient, for big ships with large draft [21]. Therefore, it will not be employed in this diploma thesis.

Another method, a bit more complex, but still possible to implement is directly integrating the Froude – Krylov pressure along of the hull of the ship. This, however requires the data for the exact shape of the hull, which is not always available [22].

Other methods for its calculation include strip theory, Computational Fluid Dynamics (CFD) and model experimentation [21, 22]. For this thesis the method suggested by the IMO Second Generation Intact Stability Criteria (SGISC) will be followed. This method is a series of empirical formulas which estimate the value of wave slope coefficient as a function of its main dimensions and its loading condition. It goes as following:

$$r = \frac{K_1 + K_2 + OG \cdot F}{\frac{B^2}{12 \cdot C_b \cdot T} - \frac{C_b \cdot T}{2} - OG}$$

Where C_b is the block coefficient and:

$$K_1 = g \cdot \beta \cdot T_r^2 \cdot (\tau + \tau \cdot \widetilde{T} - 1/\widetilde{T})/(4\pi^2)$$

$$K_2 = g \cdot \tau \cdot T_r^2 \cdot (\beta - \cos\widetilde{B})/(4\pi^2)$$

$$F = \beta \cdot (\tau - 1/\widetilde{T})$$

$$\beta = \sin(\widetilde{B})/\widetilde{B}$$

$$\tau = \exp(-\widetilde{T})/\widetilde{T}$$

$$\widetilde{B} = 2 \cdot \pi^2 \cdot B/(g \cdot T_r^2)$$

$$\widetilde{T} = 4 \cdot \pi^2 \cdot C_b \cdot d/(g \cdot T_r^2)$$

And OG is the distance of the center of gravity from the surface of water, as stated above.

Regarding the wave steepness s, its definition is:

$$s = \frac{H}{\lambda}$$

Where, H is the wave height and λ is the wavelength. Given the general lack of information about the form and shape of waves and the randomness of their appearance, the wave steepness is calculated as a function of the ship's natural roll period, according to the Table (3):

Table 3: Values of Wave Steepness

Natural roll Period, T_r (s)	**Wave Steepness, s**
≤ 6	0.100
7	0.098
8	0.093
12	0.065
14	0.053
16	0.044
18	0.038
20	0.032
22	0.028
24	0.025
26	0.023
28	0.021
≥ 30	0.020

The natural roll period is estimated earlier.

The logarithmic decrement of roll decay δ_φ is calculated as:

$$\delta_\varphi = 0.5 \cdot \pi \cdot R_{PR}$$

Where $R_{PR} = 1.87$, if the ship has a sharp bilge and otherwise given as below:

$$R_{PR} = \begin{cases} 0.17 + 0.425 \cdot \frac{100 \cdot A_k}{L_{BP} \cdot B} \text{ , if } C_{m,full} > 0.96 \\ 0.17 + (10.625 \cdot C_{m,full} - 9.775) \cdot \frac{100 \cdot A_k}{L_{BP} \cdot B} \text{ , if } 0.94 \leq C_{m,full} \leq 0.96 \\ 0.17 + 0.2125 \cdot \frac{100 \cdot A_k}{L_{BP} \cdot B} \text{ , if } C_{m,full} < 0.94 \end{cases}$$

Where A_k is the total overall area of the bilge keels (if present) in m^2 (no appendages) and $C_{m,full}$ is the midship coefficient in the fully loaded condition in calm waters.

3.1.2 Level 2 Framework

The Level 2 of the Interim Guidelines is a probabilistic assessment, taking into account irregular waves to estimate the probability of failure. As previously stated, it is advised to perform the calculations after the Level 1 assessment has shown vulnerability, but it can also be conducted, without estimating the Level 1. The objective of the guidelines is the computation of the long-term averaged probabilistic index C, which indicates the susceptibility of the ship to a specific failure type, at a certain location (usually the bridge, being the most prone to EA accidents), for a specific loading condition. Long-term index consists of a weighting factor W_i for the short-term environmental condition, and a short-term failure index $C_{S,i}$. The short-term environmental conditions are specified as a function of the significant wave height H_s and the zero-crossing wave period T_z, given by the wave scatter table [23]. The threshold for the long-term probability index is specified at 0.00039.

The criterion is described in more detail below:

Criterion Formula

In order for the ship, in a specific loading condition, to be characterized as not vulnerable, in respect of the Level 2 EA failure, the following inequality should be true:

$$C \leq R_{EA,2}$$

As stated above:

- C is the long-term probability index
- $R_{EA2} = 0.00039$

To estimate the C index the following formula is used:

$$C = \sum_{i=1}^{N} W_i \cdot C_{S,i}$$

The weighting factor W_i is given later at Table 16 according to IACS. It corresponds to the frequency of occurrence of the environmental condition i with specific significant wave height H_z and zero-crossing wave period T_z.

The short-term failure index $C_{S,i}$ represents the probability of the ship to exceed a specified lateral acceleration.

N is the total number of short-term environmental conditions as shown at Table 16.

Short-term Failure Index $C_{S,i}$

$C_{S,i}$ index calculates the rate of upcrossing a certain lateral acceleration value R_2. The linear assumption regarding roll motion, leads to a normal distribution of lateral accelerations, which makes sense given the high GM values of this failure mode. The rate of upcrossing a value of lateral acceleration, following the normal distribution, is normally given by the following formula [24]:

$$\lambda_{LA} = \frac{\sigma_{\dot{\alpha},LA}}{2\pi \cdot \sigma_{\alpha,LA}} \cdot e^{-\frac{1}{2}\left(\frac{R_2}{\sigma_{\alpha,LA}}\right)^2}$$

Where, $\sigma_{\alpha,LA}$ is the standard deviation of lateral acceleration and $\sigma_{\dot{\alpha},LA}$ is the standard deviation of a temporal of lateral acceleration. The developers of the criterion decided to ignore the effect of the fraction and keep only the exponential part. The reason behind that, is the level of difficulty in calculating the standard deviation of lateral acceleration in the frequency domain [12]. Therefore, $C_{S,i}$ is given as:

$$C_{S,i} = e^{-\frac{R_2{}^2}{2 \cdot \sigma_{LAi}{}^2}}$$

The value of the upcrossing is predefined as one g meaning that R_2 = g =9.81 m/s^2 and σ_{LAi} is the standard deviation at zero speed and in a beam seaway.

Standard Deviation of Lateral Acceleration

In order for the short-term environmental conditions to be characterized, the standard deviation of lateral acceleration is needed. To compute that, the spectrum of the sea elevation is utilized, also known as the spectral density of sea wave elevation. Generally, the spectral density of sea elevation is given by the Bretschneider spectrum. It describes the distribution of wave energy as a function of the wave frequency ω. It is given by the following formula:

$$S_{zz}(\omega) = \frac{{H_S}^2}{4\pi} \cdot \left(\frac{2\pi}{T_Z}\right)^4 \cdot \omega^{-5} \cdot e^{\left(-\frac{1}{\pi}\left(\frac{2\pi}{T_Z}\right)^4 \cdot \omega^{-4}\right)}$$

For every short-term environmental condition of the wave scatter table (pair of H_S and T_Z), the standard deviation is calculated for a number of wave frequencies. More specifically, the calculations start at the minimum frequency ω_1 and stop and the maximum frequency ω_2. The number of intervals M between that range, should not be less than 100, to ensure accuracy. In practice, for computational efficiency, the number of intervals was chosen the smallest possible, where the final result of the criterion seems to converge to a certain value. Numerous results have shown that this number can be the minimum interval count of 100, meaning that M=100. The range of the wave frequency used, are the most common to be found when at sea, taking into account the value of the natural roll period of the vessel. The formula for the square of the standard deviation of lateral acceleration is as shown below:

$${\sigma_{LAi}}^2 = \frac{3}{4} \cdot \sum_{j=1}^{M} \left(a_y(\omega_j)\right)^2 \cdot S_{zz}(\omega_j) \cdot \Delta\omega$$

Where a_y is the lateral acceleration per unit wave amplitude, so its units are $(m/s^2)/m$ and is calculated in a similar sense as the Level 1 lateral acceleration a_y. $\Delta\omega$ is the interval of wave frequency and ω_j is the midpoint of each interval, both in rad/sec. Therefore, it can easily be derived that:

$$\Delta\omega = \frac{\omega_2 - \omega_1}{M}$$

$$\omega_j = \omega_1 + \frac{2j - 1}{2} \cdot \Delta\omega$$

So, it shows that the first point of the calculations will be ($\omega_1+\Delta\omega/2$), the second ($\omega_1+3\Delta\omega/2$) and so on, until the last point (100^{th}) which will be ($\omega_1+99\Delta\omega/2$) or ($\omega_2-\Delta\omega/2$). For the lower and upper frequency limits ω_1 and ω_2 the Guidelines suggest the following values in rad/s:

$$\omega_1 = \max\left[\frac{0.5}{T_r}, 0.2\right]$$

$$\omega_2 = \min\left[\frac{25}{T_r}, 20\right]$$

Lateral Acceleration

As previously stated, the formula for lateral acceleration for the Level 2 criterion is very similar to the calculation of the Level 1 criterion. The main differences are that the wave frequency ω_j

is utilized instead of the natural roll period T_r, and the characteristic roll amplitude φ, is substituted for the roll amplitude φ_α at zero speed and in regular waves of unit amplitude, as a function of the circular frequency ω_j. Thus, φ_α is given is rad/m. So, the formula is:

$$a_y(\omega_j) = k_l \cdot (g + h_r \cdot {\omega_j}^2) \cdot \varphi_a(\omega_j)$$

Where k_l and h_r are explained at the Level 1 section. To determine the roll amplitude φ_α some empirical formulas are used. The roll amplitude is considered to be a combination of two separate roll angles φ_r and φ_i, connected with the formula:

$$\varphi_a(\omega_j) = \sqrt{\varphi_r(\omega_j)^2 + \varphi_i(\omega_j)^2}$$

Where the two new roll angles are given as:

$$\varphi_r(\omega_j) = \frac{a \cdot (\rho \cdot g \cdot \nabla \cdot GM - J_{T,roll} \cdot {\omega_j}^2) + b \cdot B_e \cdot \omega_j}{(\rho \cdot g \cdot \nabla \cdot GM - J_{T,roll} \cdot {\omega_j}^2)^2 + (B_e \cdot \omega_j)^2}$$

$$\varphi_i(\omega_j) = \frac{b \cdot (\rho \cdot g \cdot \nabla \cdot GM - J_{T,roll} \cdot {\omega_j}^2) - a \cdot B_e \cdot \omega_j}{(\rho \cdot g \cdot \nabla \cdot GM - J_{T,roll} \cdot {\omega_j}^2)^2 + (B_e \cdot \omega_j)^2}$$

Where:

- $\rho = 1.025$ t/m^3: the density of salt water
- ∇: the volume of displacement at the design draft (m^3)
- a and b: cosine and sine components of Froude – Krylov roll moment, respectively, in regular beam waves of unit amplitude (kN·m/m)
- $J_{T,roll}$: roll moment inertia comprising added inertia (t·m^2)
- B_e: equivalent roll damping factor (kN·m·s)

The Froude – Krylov roll moment components can be directly calculated by integrating the undisturbed linear wave pressure over the wetted surface. However, for lateral symmetric ship hulls the following approximation can be used:

$$a = 0$$

$$b = \Delta \cdot GM \cdot r \cdot {\omega_j}^2$$

Where, Δ is the displacement of the ship in tonnes and r is the wave slope coefficient as computed in Level 1 criterion.

For the roll moment inertia, given the lack of sufficient information, the following formula can be applied:

$$J_{T,roll} = \frac{\rho \cdot g \cdot \nabla \cdot GM \cdot {T_r}^2}{4\pi^2}$$

The equivalent linear roll damping factor is given as:

$$B_e = 2 \cdot J_{T,roll} \cdot \mu_e$$

Where μ_e is the equivalent roll damping coefficient. There are various other ways to calculate the roll damping data, such as the roll damping coefficient and damping factor. Some of them include model experiments and the simplified Ikeda method. However, given the complexity in these predictions, a satisfying approximation that adequately represents real-world conditions, and also, doesn't underestimate the final result of the criterion, is $\mu_e = 0.03$.

3.2 Cargo Securing Manual Framework

The Annex 2 of IMO's Code of Safe Practice for Cargo Stowage and Security (CSS code) contains specific guidelines for the making of the Cargo Securing Manual (CSM). As stated before, the CSM has to contain all the essential information for the ship Captain, regarding the safety and the protection of the cargo [1]. It has to be consistent, with other requirements like the trim and stability booklet, Load Line Certificate and the Loading Manual, and be approved by a classification society. It always has to be onboard, for the Master to access or for authorities to examine it [25].

Specifically for containers, it's called Container Securing Manual. It involves among other information the following [25]:

- Container Arrangement Plan and the numbering for all the containers
- Capacity plan, showing all the slots for container stowage
- Visibility restrictions, depending on the draft and trim
- A list with all the securing devices available on board and the correct way to install them
- The strength of the lashings
- The weight that each container can carry
- Computation methods that calculate the forces that can develop on the lashings depending on the weather and ship's movement

The calculations for the forces developed at the lashings are going to be conducted, according to the Guidelines of the Chinese Classification Society CR [25]. These forces are greatly affected by the movement of the ship and its lateral acceleration. The method for calculating these accelerations is going to be compared with the respective method of the SGISC.

3.2.1 Roll and Pitch Movement Characteristics

The first step of the calculations is to estimate the ship's natural roll period and the roll angle. Obviously, the estimates described in the SGISC can be utilized as well, but CSM suggests different formulas. These estimates only take into account the main dimensions of the ship, so

it's possible their precision is lower that the SGISC's. For the natural roll period and the roll angle (in degrees), respectively the formulas are the following:

$$T_r = \frac{0.8 \cdot B}{\sqrt{GM}}$$

$$\varphi = \frac{3150 \cdot C}{B + 75}$$

Where, if the ship has bilge keels:

$$C = \begin{cases} 0.75 \text{ , if } T_r \leq 18 \text{ sec} \\ 0.75 + 0.1 \cdot (18 - T_r) \text{ , if } T_r \geq 18 \text{ sec} \end{cases} \text{, with a maximum value for } C = 0.9$$

Otherwise, if the ship doesn't have bilge keels, C=1.

For the roll center R_{CTR}, or roll axis as referred at in the SGISC, instead of the midpoint between the center of gravity and the waterline (like suggested in the SGISC), it's simply taken at the center of gravity. If the center of gravity is not known precisely, the following formula is suggested:

$$R_{CTR} = \frac{D}{4} + \frac{T}{2}$$

Measured in meters from the baseline, where D is the molded depth at the sides.

The Guidelines calculate the pitch acceleration as well, in order to fully check the security of the containers. The formulas for the pitch movement will be written below, to present the method completely. However, no calculations will be made in later chapters.

The CSS Guidelines propose some typical values, usually found in ships, for the pitch angle θ and the pitch period T_P, depending on the ship's length. The pitch center should be taken at the Longitudinal Center of Floatation (LCF) and if it's not known, the estimation below should be followed:

$$\theta = \begin{cases} 7 \text{ degrees, if } L_{BP} \leq 120 \text{ m} \\ 6 \text{ degrees, if } 120 \text{ m} < L_{BP} < 275 \text{ m} \\ 5 \text{ degrees, if } L_{BP} \geq 275 \text{ m} \end{cases}$$

$$T_P = 7 + 0.0123 \cdot (L_{BP} - 183)$$

$$P_{CTR} = 0.4 \cdot L_{BP}$$

3.2.2 Accelerations

After determining the roll and pitch angles and periods, the accelerations developed on the ship can also be estimated. The guidelines are referring to two different conditions, Condition A and Condition B. The securing system should be able to withstand the forces that are generated in both conditions. Condition A is characterized by maximum roll accelerations, and is expected in beam and quartering to stern seas. Condition B has maximum pitch accelerations and is expected in head or almost head waves. For containers that are stowed on deck with lashing systems according to the Guidelines, only Condition A has to be evaluated. For containers that are stowed in cell guides, only Condition B has to be evaluated. In this thesis, as previously stated, only Condition A will be examined and Condition B results are not going to be included.

In order to check the strength of lashing of all containers, the location of every container should be known. Their location is described with three parameters, x_C, y_C and z_C for the longitudinal, transverse and vertical position, respectively, showing the center of gravity of each container from the aft perpendicular and the baseline. However, the distances, $|x_C - P_{CTR}|$ and $|z_C - R_{CTR}|$ from the roll and pitch center are going to be used for the calculation of the accelerations, as shown in the Figures 8 and 9.

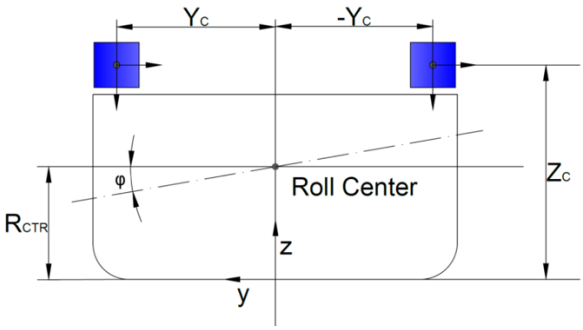

Figure 8: Distance from Roll Center [25]

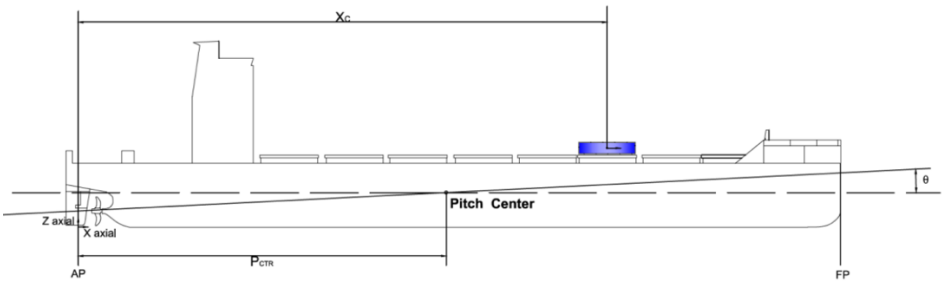

Figure 9: Distance from Pitch Center [25]

To calculate the accelerations the following two parameters are needed, for both conditions. The common acceleration parameter a_0 in g's, and the force factor k_3, taking into account the longitudinal position of the container stack, similar to k_L in the SGISC:

$$a_0 = \begin{cases} 0.2012 \text{ , for B} \leq 32.2 \text{ m} \\ 0.2012 + \dfrac{(0.0618 \cdot \sqrt{GM} - 0.2125) \cdot (B - 32.2)}{7.8} \text{ , for } 32.2 \text{ m} < B < 40 \text{ m} \\ 0.1417 + 0.0618 \cdot \sqrt{GM} - 0.0038 \cdot B \text{ , for B} \geq 40 \text{ m} \end{cases}$$

$$k_3 = \begin{cases} 0.5 \cdot \left(\dfrac{0.2 \cdot L_{BP} - x_c}{0.2 \cdot L_{BP}}\right) \text{ , for } x_c \leq 0.2 \cdot L_{BP} \\ 0 \text{ , for } 0.2 \cdot L_{BP} < x_c < 0.7 \cdot L_{BP} \\ 0.7 \cdot \left(\dfrac{x_c - 0.7 \cdot L_{BP}}{0.3 \cdot L_{BP}}\right) \text{ , for } x_c \geq 0.7 \cdot L_{BP} \end{cases}$$

So, for Condition A the traverse acceleration, A_T is given in g's below. The maximum and minimum vertical accelerations A_{VMAX} and A_{VMIN} are given in the Guidelines, also in g's. The maximum value for A_{VMIN} is taken as 1·g:

$$A_T = a_{GT} + k_C \cdot a_{RT} + (1 + k_3) \cdot a_0 \cdot \sin\varphi$$

$$A_{VMAX} = a_{GRV} + k_C \cdot a_{RV} + (1 + k_3) \cdot a_0 \cdot \cos\varphi$$

$$A_{VMIN} = a_{GRV} - k_C \cdot a_{RV} + (1 - k_3) \cdot a_0 \cdot \cos\varphi$$

Where:

- $a_{GT} = \sin\varphi$: transverse static gravitational acceleration component in g's
- $a_{RT} = \frac{\varphi}{T_r{}^2} \cdot |z_c - R_{CTR}|$: transverse roll acceleration component in g's
- $a_{GRV} = \cos\varphi$: vertical static gravitational acceleration component in g's
- $a_{GT} = \frac{\varphi}{T_r{}^2} \cdot |y_c|$: vertical roll acceleration component in g's
- $k_C = 0.0701$, when x_C, y_C, z_C are in meters

Similarly, for Condition B the longitudinal acceleration A_L, the maximum vertical acceleration A_{VMAX} and the minimum vertical acceleration A_{VMIN} are only mentioned, for the sake of completeness:

$$A_L = a_{GL} + k_C \cdot a_{PL} + a_0 \cdot \sin\theta$$

$$A_{VMAX} = a_{GPV} + k_C \cdot a_{PV} + a_0 \cdot \cos\theta$$

$$A_{VMIN} = a_{GPV} - k_C \cdot a_{PV} + a_0 \cdot \cos\theta$$

Where:

- $a_{GL} = \sin\theta$: longitudinal static gravitational acceleration component in g's
- $a_{PL} = \frac{\theta}{T_r{}^2} \cdot |z_c - R_{CTR}|$: longitudinal pitch acceleration component in g's

- $a_{GPV} = \cos\theta$: vertical static gravitational acceleration component in g's
- $a_{PV} = \frac{\theta}{T_p{}^2} \cdot |x_c - P_{CTR}|$: vertical pitch acceleration component in g's

3.2.3 Loads Acting on Containers

All the forces acting on the containers are shown in Figure 10.

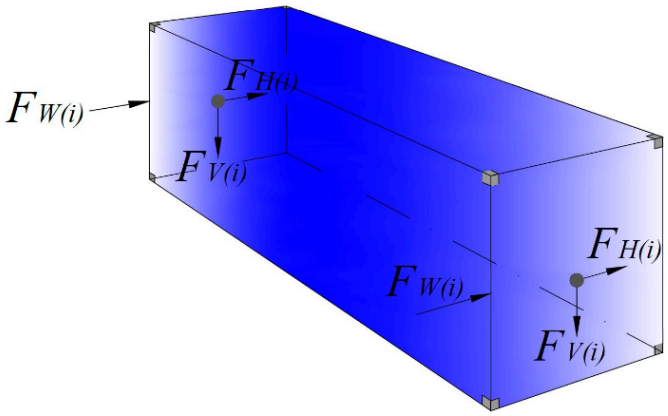

Figure 10: Forces acting on the sides of the container [25]

The horizontal force component F_H and the vertical force component F_V, acting on the containers, due to gravity and the movements of the ship are given in the following formulas:

$$F_H = 0.5 \cdot W \cdot A_T$$

$$F_V = \begin{cases} 0.5 \cdot W \cdot A_{V,max} \text{ , when evaluating corner post compression} \\ 0.5 \cdot W \cdot A_{V,min} \text{ , when evaluating corner post tension} \end{cases}$$

Where W is the weight of each container in kN, given from each time from the loading condition.

The wind load F_W on each container is taken as:

$$F_W = 0.5 \cdot P_W \cdot L_C \cdot H_C$$

Where P_W is the wind pressure taken as constant and equal to 1.08 kN/m^2, L_C is the length of the container and H_C is its height. It's assumed that 50% of the wind force is acting on top of the container and 50% at the bottom.

The transverse force or racking force Q_i acting on top the container in tier i, if no transverse lashings are present is given by the formula, kN:

$$Q_i = r_T \cdot F_{H,i} + r_W \cdot F_{W,i} + \sum_{j=i+1}^{n} (F_{H,j} + F_{W,j})$$

Where:

- n is the number of tiers on the stack getting examined
- r_T is the portion of horizontal force F_H, contributing on the racking force, assumed to be equal to 0.45
- r_W is the portion of wind force F_W, contributing on the racking force, assumed to be equal to 0.5

3.2.4 Lashing Data

In order to calculate the forces acting on the lashings, some of their characteristics, regarding their geometry and their material should be known. Firstly, the lashing spring constant K_l should be calculated by using load/strain tests. When that's not possible, it can be calculated from the stiffness of the tension element. A tension element can be a wire, rod or a chain and its stiffness is given as, in kN/mm:

$$K_l = \frac{A_l \cdot E_l}{L_l}$$

Where A_l is the cross – sectional area of the lashing tension element in mm^2, E_l is the equivalent elastic modulus in GPa and L_l is the lashing's length, from the securing point to the container's corner in mm. For lashings made of steel, the Guidelines provide the following tables for the cross – sectional area (Table 4) and the elastic modulus (Table 5):

Table 4: Lashings' Cross – Sectional Area

Lashing Element	A_l
Steel Wire Rope	Nominal area
Steel Rod	Actual area
Steel Chain	One side of link

Table 5: Lashings' Elastic Modulus

Lashing Element	E_l (kN/mm^2)
Steel Wire Rope	88.3
Steel Rod in lashing assembly with L$l \leq$ 5000 mm (for lashings extending up ~1 tier)	97.1
Steel Rod in lashing assembly with L$l >$ 5000 mm (for lashings extending up ~2 tiers)	176.6
Steel Chain	98.1

For the calculations the elastic modulus of the steel rod is going to be used. The lashing's length can be given from the formula:

$$L_l = \sqrt{{L_x}^2 + {L_y}^2 + {L_z}^2}$$

Where L_x, L_y and L_z are the longitudinal, transverse and vertical extent of the lashing, respectively, as shown in Figure 11. L_x is usually very small, so it can be taken as zero in the above formula. L_y and L_z are taken equal to the corresponding dimensions of the container, according to ISO standards.

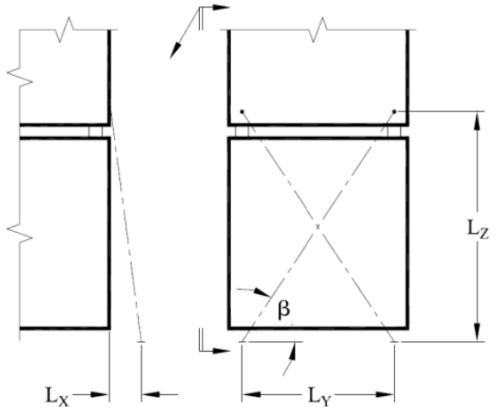

Figure 11: Lashing's Length

The horizontal component K_{lH} of the lash spring constant is also needed and it's expressed as:

$$K_{lH} = K_l \cdot \cos\beta^2$$

Where β is the lash angle of mooring in degrees, as shown in Figure 11.

When a load is acting upon a lashing element, it should not exceed a certain value in order to be considered safe. This value is the Safe Working Load (SWL) and is taken as the 50-60% of the Minimum Breaking Strength (MBS), for all securing fittings. Typical values for the SWL and MBS for steel fittings are given at Table 6:

Table 6: Securing Elements Typical Strength

Lashing Element	MBS (kN)	SWL (kN)
Tension Element (Lashing Rod)	490	293
Tensioning Device (Turnbuckle)	490	293
Lock Fitting (Twistlock)	500	299
Lashing Point (Lashing Plate)	490	293
Lashing Point (D-Ring)	460	275
Twistlock Foundation (Base Socket)	500	299
TP Bridge Fitting	400	200

For the calculations following in this thesis, the value for the Lashing Rod (SWL = 293 kN) is of interest. A Safety Factor (SF) also has to be utilized to ensure the safe and steady operation of the lashings. A typical value for the Safety Factor is 1.5 and after being applied to the SWL, the Calculated Strength (CS) is given:

$$\mathrm{CS} = \frac{\mathrm{SWL}}{\mathrm{SF}} = 195.33\ \mathrm{kN}$$

3.2.5 Forces Acting of Lashings

Two typical lashing arrangements are going to be examined, single cross lash to deck and double cross lash to deck in a 3 tier stack, as shown in Figures 12 and 13.

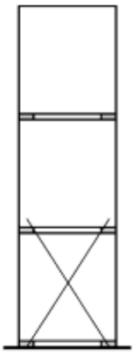

Figure 12: Single Lashing to Deck

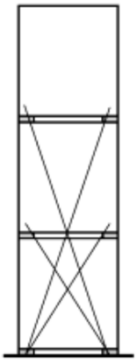

Figure 13: Double Lashing to Deck

For the first case the horizontal force component of the lashing $F_{lH,1}$ is:

$$F_{lH,1} = Q_1 \cdot \left(\frac{K_{lH,1}}{K_{C1}+K_{lH1}}\right)$$

Where Q_1 is the racking force of the bottom container, as calculated previously, K_{lH1} is the horizontal component of the spring constant K_l of the (first) lashing and K_{C1} is the racking spring constant of the first container. The racking spring constant is given in the Table 7:

Table 7: Racking Spring Constant

Panel Location	Container Racking Spring Constant (kN/mm)
Container Door End, K_C	3.73
Container Closed End, K_C	15.69
Container Side, K_{CL}	5.79

For the racking spring constant, the smaller value is going to be used, which is the one that leads to the most adverse results. This is the spring constant for the door end of the container.

For the second, F_{lH} for both lashings:

$$F_{lH,1} = K_{lH,1} \cdot \left(\frac{(Q_1 - Q_2) \cdot K_{lH,2} + Q_1 \cdot K_{C2}}{(K_{C1} + K_{lH1}) \cdot (K_{C2} + K_{lH2}) + K_{C2} \cdot K_{lH2}} \right)$$

$$F_{lH,2} = K_{lH,2} \cdot \left(\frac{K_{C2} \cdot Q_1 + Q_2 \cdot K_{C1} + Q_2 \cdot K_{lH1}}{(K_{C1} + K_{lH1}) \cdot (K_{C2} + K_{lH2}) + K_{C2} \cdot K_{lH2}} \right)$$

Obviously, in order to find the tension T_l acting for all the lashings, the horizontal forces have to be divided with the cosine of the lash angle β. Meaning:

$$T_l = \frac{F_{lH}}{\cos\beta}$$

The tension T_l, then has to be compared to the CS in order to verify if the stowage of the containers is secured. Meaning that if:

$$T_l \leq CS$$

Then the stowing system is secured.

Chapter 4: Application of the Regulations

In this chapter, the guidelines for Level 1 and Level 2 of the EA criterion and the CSM, are applied to a model ship. The calculations are performed for four loading conditions, in order to get a wider picture of the criteria. For each of the four loading conditions, that were chosen, the process analyzed in Chapter 3 was followed and the necessary mathematical calculations were conducted. The results will be presented in matrices and the criteria will be checked if they are satisfied. It is important to be mentioned, that all the results, matrices and graphs presented below were generated using the Wolfram Mathematica programming language.

4.1 Main Characteristics and Loading Conditions of the Ship

The model ship is a Post-Panamax Container Carrier with a maximum capacity of around 4900 20-inch TEU. The ship contains 7 cargo holds and 13 hatches, capable of carrying more containers, on deck. It has a bulbous bow and a pair of bilge keels. The body plan of the vessel is shown in Figure 14. Its main dimensions as long as the characteristics of each Loading Condition (LC) are shown in Tables 8 and 9, respectively.

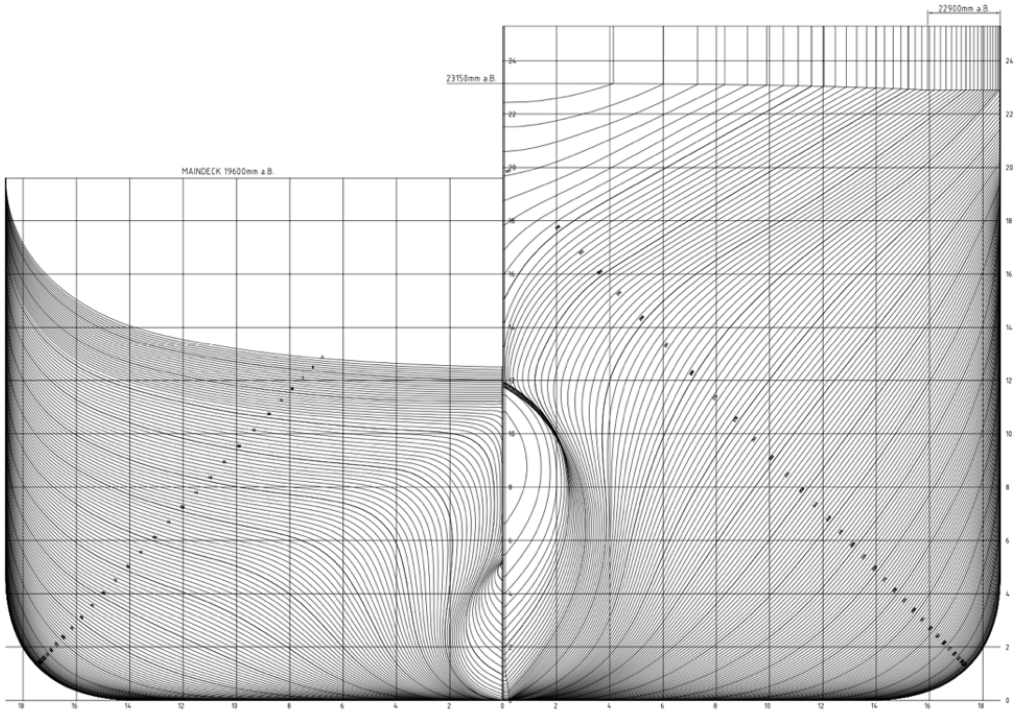

Figure 12: Model Ship Body Plan

Table 8: Main Dimensions

Particulars	Symbol	Value
Length Overall	L_{OA} (m)	250
Length Between Perpendiculars	L_{BP} (m)	238.35
Moulded Breadth	B (m)	37.3
Moulded Depth	D (m)	19.6
Design Draught	T_d (m)	11.5
Displacement at Design Draught	Δ_d (t)	68014

Table 9: Loading Conditions Characteristics

Characteristics	Symbol	Loading Conditions			
		21	30	36	39
Number of TEU	-	2770	3262	2659	2366
Container Homogenous Weight	homo (t)	18	12	16	18
Waterline Length	L_{WL} (m)	242.05	248.59	248.59	248.59
Draught	T (m)	12.52	11.52	11.52	11.52
Displacement	Δ (t)	75850.1	68192.8	68199.1	68013.1
Volume of Displacement	∇ (m^3)	74000.1	66529.6	66535.7	66354.2
Block Coefficient	C_b	0.663	0.647	0.647	0.647
Midship Coefficient	C_m	0.983	0.981	0.981	0.981
Vertical Center of Gravity	KG (m)	15.28	15.62	14.83	14.21
Metacentric Height	GM (m)	2.36	2.05	2.85	3.42

The loading conditions with the highest GM values are chosen, in order to examine the most severe situations, regarding the developed lateral accelerations.

Moreover, the longitudinal and vertical location of the bridge deck are required, as this is the area where the EA criterion will be assessed, as explained earlier. The area of the bilge keels, if present, is also needed. In the model ship plans both information are accessible. The bridge deck can be located from the General Arrangement (GA) and for the bilge keels the length and width ratios (l_{BK} and b_{BK} respectively) are:

$$l_{BK} = 0.3 \cdot L_{BP}$$

$$b_{BK} = 0.011 \cdot B$$

The longitudinal position of the bridge deck is taken at the end closer to the Aft Perpendicular (AP), in order to take into account, the pitch and yaw motions, with the use of k_l factor, and assess the most severe situation. The longitudinal distance from the AP and the vertical distance from the Baseline (BL) of the bridge deck, as long as the area of the bilge keels are shown in Table 10:

Table 10: Bridge Deck and Bilge Keels Characteristics

Particulars	Symbol	Value
Bridge Deck Longitudinal Distance	x (m)	41
Bridge Deck Vertical Distance	h_k (m)	45
Bilge Keel Length	l_{BK} (m)	71.5
Bilge Keel Width	b_{BK} (m)	0.41
Bilge Keel Area	A_k (m^2)	58.63

4.2 Level 1 EA Criterion Application

Firstly, the calculations for the initial particulars of the criterion can be made and the results are shown in Table 11:

Table 11: Initial Calculations

Particulars	Loading Conditions			
	21	30	36	39
h_{roll} (m)	13.9	13.57	13.18	12.87
h_r (m)	31.1	31.43	31.82	32.14
C	0.337	0.341	0.341	0.341
T_r (s)	16.39	17.75	15.05	13.74
s	0.0428	0.0388	0.0483	0.0546
k_l	1.0175	1.0175	1.0175	1.0175

In the Table 12, the results of the process for the calculation the wave slope coefficient, r, are presented:

Table 12: Wave Slope Coefficient Calculation

Particulars	Loading Conditions			
	21	30	36	39
OG (m)	2.76	4.1	3.31	2.69
$\widetilde{B}$	0.280	0.238	0.331	0.398
$\widetilde{T}$	0.124	0.095	0.132	0.159
β	0.987	0.991	0.982	0.974
τ	7.098	9.544	6.615	5.368
F	-0.928	-0.945	-0.920	-0.900
K_1	-3.77	-3.47	-3.35	-3.27
K_2	12.24	14.06	13.48	13.06
r	**0.837**	**0.870**	**0.831**	**0.807**

For all four loading conditions R_{PR} and the decrement of roll decay, $\delta\varphi$, are the same and equal to (for $C_m > 0.94$):

$$R_{PR} = 0.450$$

$$\delta\varphi = 0.707$$

So, all the necessary information is computed, in order to determine the roll amplitude, φ, and then the lateral acceleration, a_y, showing if the criterion is satisfied.

Table 13: Roll Amplitude and Lateral Acceleration

Particulars	**Loading Conditions**			
	21	**30**	**36**	**39**
φ (rad)	0.189	0.178	0.211	0.232
φ (degrees)	10.82	10.18	12.11	13.29
a_y (m/s^2)	2.76	2.49	3.30	3.90
Status	**Pass**	**Pass**	**Pass**	**Pass**

A quick look at the results in Table 13, and comparing the acceleration with the criterion upper limit $R_{EA1} = 4.64$ m/s^2, it's obvious, that the model ship passes the Level 1 EA criterion for all the loading conditions. This means that Level 2 calculations are not required to be carried out. However, they will be performed, regardless, to verify the consistency of the results.

4.3 Level 2 EA Criterion Application

For the application of the Level 2 criterion, a proper value for the wave frequency interval, $\Delta\omega$, has to be determined, in order to give satisfying results for the standard deviation, σ_{LAi}. According to the Guidelines suggestions, the values for the wave frequency interval and the lower and upper wave frequency limit, ω_1 and ω_2, respectively, are shown in Table 14:

Table 14: Wave Frequencies

Frequencies	**Loading Conditions**			
	21	**30**	**36**	**39**
$\Delta\omega$ (rad/s)	0.01326	0.01209	0.01461	0.01620
ω_1 (rad/s)	0.200	0.200	0.200	0.200
ω_2 (rad/s)	1.526	1.409	1.661	1.820

The roll moment of inertia $J_{T,roll}$ and the equivalent linear roll damping factor B_e are in Table 15:

Table 15: Roll Moment of Inertia and Linear Roll Damping Factor

Frequencies	**Loading Conditions**			
	21	**30**	**36**	**39**
$J_{T,roll}$ (t·m^2)	1.19E+07	1.094E+07	1.094E+07	1.091E+07
B_e (kN·m·s)	7.166E+06	6.563E+06	6.564E+06	6.546E+06

As previously stated, the Level 2 criterion utilizes a wave scatter table, suggested by IACS in 2001, to define the possibility of occurrence of each environmental condition. This possibility is expressed as a weighting factor W_i for the long term probability index. The data were collected by observations made in the North Atlantic, for a total of ten thousand occurrences. Due to some criticism, recently, the scatter diagram was updated by IACS, in 2023 [26]. The new table uses more precise methods and a wider geographical area to calculate each environmental occurrence. However, for now the older table found in the IMO Guidelines [11] will be used. The wave scatter table is shown in Table 16:

Table 16: IACS Wave Scatter Table

T_z (s) → / **H_S (m) ↓**	**3.5**	**4.5**	**5.5**	**6.5**	**7.5**	**8.5**	**9.5**	**10.5**	**11.5**	**12.5**	**13.5**	**14.5**	**15.5**	**16.5**	**17.5**	**18.5**
0.5	1.3	133.7	865.6	1186	634.2	186.3	36.9	5.6	0.7	0.1	0	0	0	0	0	0
1.5	0	29.3	986.0	4976.0	7738.0	5569.7	2375.7	703.5	160.7	30.5	5.1	0.8	0.1	0	0	0
2.5	0	2.2	197.5	2158.8	6230.0	7449.5	4860.4	2066.0	644.5	160.2	33.7	6.3	1.1	0.2	0	0
3.5	0	0.2	34.9	695.5	3226.5	5675.0	5099.1	2838.0	1114.1	337.7	84.3	18.2	3.5	0.6	0.1	0
4.5	0	0	6.0	196.1	1354.3	3288.5	3857.5	2685.5	1275.2	455.1	130.9	31.9	6.9	1.3	0.2	0
5.5	0	0	1.0	51.0	498.4	1602.9	2372.7	2008.3	1126.0	463.6	150.9	41.0	9.7	2.1	0.4	0.1
6.5	0	0	0.2	12.6	167.0	690.3	1257.9	1268.6	825.9	386.8	140.8	42.2	10.9	2.5	0.5	0.1
7.5	0	0	0	3.0	52.1	270.1	594.4	703.2	524.9	276.7	111.7	36.7	10.2	2.5	0.6	0.1
8.5	0	0	0	0.7	15.4	97.9	255.9	350.6	296.9	174.6	77.6	27.7	8.4	2.2	0.5	0.1
9.5	0	0	0	0.2	4.3	33.2	101.9	159.9	152.2	99.2	48.3	18.7	6.1	1.7	0.4	0.1
10.5	0	0	0	0	1.2	10.7	37.9	67.5	71.7	51.5	27.3	11.4	4.0	1.2	0.3	0.1
11.5	0	0	0	0	0.3	3.3	13.3	26.6	31.4	24.7	14.2	6.4	2.4	0.7	0.2	0.1
12.5	0	0	0	0	0.1	1.0	4.4	9.9	12.8	11.0	6.8	3.3	1.3	0.4	0.1	0
13.5	0	0	0	0	0	0.3	1.4	3.5	5.0	4.6	3.1	1.6	0.7	0.2	0.1	0
14.5	0	0	0	0	0	0.1	0.4	1.2	1.8	1.8	1.3	0.7	0.3	0.1	0	0
15.5	0	0	0	0	0	0	0.1	0.4	0.6	0.7	0.5	0.3	0.1	0.1	0	0
16.5	0	0	0	0	0	0	0	0.1	0.2	0.2	0.2	0.1	0.1	0	0	0

Dividing each cell of Table 16 with 10000, you get the probability of occurrence or the W_i factor, for every environmental condition.

In the following Tables, the results for each loading condition are presented. More specifically, they include the standard deviation (σ_{LAi}), the short-term failure index ($C_{S,i}$) and the weighted average of the short-term environmental conditions ($C_{S,i} \cdot W_i$), the sum of which makes up the long-term probability index (C), as explained earlier. Values lower than 10^{-100}, were neglected and put as zeroes in all the matrices. Higher values could also be neglected, without affecting the final result, but were included, for the sake of completeness.

4.3.1 Level 2 Results for LC21

Table 17: Standard Deviations σ_{LAi} for LC21

T_z (s) → / H_S (m) ↓	3.5	4.5	5.5	6.5	7.5	8.5	9.5	10.5	11.5	12.5	13.5	14.5	15.5	16.5	17.5	18.5
0.5	0.068	0.070	0.064	0.059	0.058	0.061	0.068	0.073	0.075	0.074	0.071	0.067	0.062	0.057	0.053	0.048
1.5	0.203	0.209	0.192	0.177	0.173	0.184	0.205	0.220	0.226	0.222	0.213	0.200	0.186	0.171	0.158	0.145
2.5	0.339	0.348	0.320	0.296	0.288	0.307	0.341	0.367	0.376	0.370	0.354	0.333	0.309	0.286	0.263	0.242
3.5	0.475	0.488	0.449	0.414	0.404	0.430	0.477	0.514	0.527	0.518	0.496	0.466	0.433	0.400	0.368	0.338
4.5	0.610	0.627	0.577	0.532	0.519	0.553	0.614	0.661	0.678	0.667	0.638	0.599	0.557	0.514	0.473	0.435
5.5	0.746	0.766	0.705	0.651	0.634	0.675	0.750	0.808	0.828	0.815	0.779	0.732	0.680	0.628	0.578	0.532
6.5	0.882	0.905	0.833	0.769	0.749	0.798	0.886	0.955	0.979	0.963	0.921	0.865	0.804	0.743	0.684	0.629
7.5	1.017	1.045	0.961	0.887	0.865	0.921	1.023	1.102	1.129	1.111	1.063	0.998	0.928	0.857	0.789	0.725
8.5	1.153	1.184	1.089	1.006	0.980	1.044	1.159	1.249	1.280	1.259	1.204	1.131	1.051	0.971	0.894	0.822
9.5	1.289	1.323	1.218	1.124	1.095	1.167	1.295	1.395	1.430	1.407	1.346	1.265	1.175	1.085	0.999	0.919
10.5	1.424	1.463	1.346	1.242	1.211	1.290	1.432	1.542	1.581	1.555	1.488	1.398	1.299	1.199	1.104	1.015
11.5	1.560	1.602	1.474	1.361	1.326	1.412	1.568	1.689	1.732	1.704	1.629	1.531	1.422	1.314	1.209	1.112
12.5	1.695	1.741	1.602	1.479	1.441	1.535	1.704	1.836	1.882	1.852	1.771	1.664	1.546	1.428	1.315	1.209
13.5	1.831	1.881	1.730	1.597	1.556	1.658	1.841	1.983	2.033	2.000	1.913	1.797	1.670	1.542	1.420	1.306
14.5	1.967	2.020	1.859	1.716	1.672	1.781	1.977	2.130	2.183	2.148	2.054	1.930	1.794	1.656	1.525	1.402
15.5	2.102	2.159	1.987	1.834	1.787	1.904	2.114	2.277	2.334	2.296	2.196	2.063	1.917	1.771	1.630	1.499
16.5	2.238	2.298	2.115	1.952	1.902	2.026	2.250	2.424	2.484	2.444	2.338	2.196	2.041	1.885	1.735	1.596

Table 18: Short Term Failure Index $C_{S,i}$ for LC21

T_z (s) → / H_S (m) ↓	3.5	4.5	5.5	6.5	7.5	8.5	9.5	10.5	11.5	12.5	13.5	14.5	15.5	16.5	17.5	18.5
0.5	0	0	0	0	0	0	0	0	0	0	0	0	0	0	0	0
1.5	0	0	0	0	0	0	0	0	0	0	0	0	0	0	0	0
2.5	0	0	0	0	0	0	0	0	0	0	0	0	0	0	0	0
3.5	1.9E-93	1.2E-88	0	0	0	0	1.8E-92	8.6E-80	5.6E-76	1.8E-78	1.1E-85	5.2E-97	0	0	0	0
4.5	8.1E-57	6.6E-54	1.5E-63	1.9E-74	2.3E-78	3.8E-69	3.1E-56	1.5E-48	3.0E-46	9.4E-48	3.9E-52	5.7E-59	3.6E-68	8.3E-80	5E-94	0
5.5	2.8E-38	2.5E-36	8.9E-43	4.5E-50	1.1E-52	1.6E-46	7.0E-38	9.6E-33	3.4E-31	3.3E-32	3.9E-35	1.0E-39	7.1E-46	1.2E-53	3.5E-63	1.4E-74
6.5	1.3E-27	3.2E-26	7.8E-31	4.6E-36	6.2E-38	1.6E-33	2.5E-27	1.2E-23	1.5E-22	2.9E-23	2.3E-25	1.2E-28	4.7E-33	1.3E-38	1.9E-45	1.3E-53
7.5	6.4E-21	7.2E-20	2.4E-23	2.9E-27	1.1E-28	2.3E-25	1.0E-20	6.0E-18	4.1E-17	1.2E-17	3.1E-19	1.1E-21	5.2E-25	3.4E-29	2.6E-34	1.9E-40
8.5	1.9E-16	1.2E-15	2.5E-18	2.2E-21	1.7E-22	6.7E-20	2.8E-16	3.9E-14	1.7E-13	6.6E-14	3.9E-15	4.7E-17	1.2E-19	6.9E-23	7.1E-27	1.2E-31
9.5	2.6E-13	1.2E-12	8.1E-15	2.9E-17	3.8E-18	4.4E-16	3.5E-13	1.9E-11	6.1E-11	2.8E-11	2.9E-12	8.5E-14	7.3E-16	1.8E-18	1.2E-21	1.7E-25
10.5	5.0E-11	1.7E-10	2.9E-12	2.9E-14	5.5E-15	2.7E-13	6.4E-11	1.6E-09	4.4E-09	2.3E-09	3.6E-10	2.0E-11	4.1E-13	3.0E-15	7.3E-18	5.4E-21
11.5	2.6E-09	7.2E-09	2.4E-10	5.2E-12	1.3E-12	3.3E-11	3.2E-09	4.7E-08	1.1E-07	6.3E-08	1.3E-08	1.2E-09	4.7E-11	7.8E-13	5.2E-15	1.3E-17
12.5	5.4E-08	1.3E-07	7.2E-09	2.8E-10	8.7E-11	1.4E-09	6.4E-08	6.3E-07	1.3E-06	8.0E-07	2.2E-07	2.8E-08	1.8E-09	5.6E-11	8.1E-13	5.0E-15
13.5	5.9E-07	1.2E-06	1.0E-07	6.4E-09	2.4E-09	2.5E-08	6.8E-07	4.8E-06	8.8E-06	6.0E-06	1.9E-06	3.4E-07	3.2E-08	1.6E-09	4.3E-11	5.5E-13
14.5	4.0E-06	7.5E-06	8.9E-07	7.9E-08	3.3E-08	2.6E-07	4.5E-06	2.5E-05	4.1E-05	3.0E-05	1.1E-05	2.5E-06	3.2E-07	2.4E-08	1.0E-09	2.4E-11
15.5	1.9E-05	3.3E-05	5.1E-06	6.1E-07	2.9E-07	1.7E-06	2.1E-05	9.3E-05	1.5E-04	1.1E-04	4.6E-05	1.2E-05	2.1E-06	2.2E-07	1.4E-08	5.0E-10
16.5	6.7E-05	1.1E-04	2.1E-05	3.3E-06	1.7E-06	8.1E-06	7.4E-05	2.8E-04	4.1E-04	3.2E-04	1.5E-04	4.7E-05	9.6E-06	1.3E-06	1.1E-07	6.2E-09

Table 19: Long Term Failure Index Components $C_{S,i} \cdot W_i$ for LC21

T_z (s) → / H_S (m) ↓	3.5	4.5	5.5	6.5	7.5	8.5	9.5	10.5	11.5	12.5	13.5	14.5	15.5	16.5	17.5	18.5
0.5	0	0	0	0	0	0	0	0	0	0	0	0	0	0	0	0
1.5	0	0	0	0	0	0	0	0	0	0	0	0	0	0	0	0
2.5	0	0	0	0	0	0	0	0	0	0	0	0	0	0	0	0
3.5	0	2.4E-94	0	0	0	0	9.0E-94	2.5E-81	6.3E-78	6.1E-81	8.9E-89	0	0	0	0	0
4.5	0	0	9.2E-68	3.7E-77	3.2E-80	1.3E-70	1.2E-57	4.0E-50	3.8E-48	4.3E-50	5.2E-55	1.8E-62	2.5E-72	1.1E-84	1.0E-99	0
5.5	0	0	8.9E-48	2.3E-53	5.4E-55	2.5E-48	1.7E-39	1.9E-34	3.8E-33	1.5E-34	5.8E-38	4.2E-43	6.8E-50	2.4E-58	1.4E-68	1.4E-80
6.5	0	0	1.6E-36	5.8E-40	1.0E-40	1.1E-35	3.1E-29	1.5E-25	1.3E-24	1.1E-25	3.2E-28	5.1E-32	5.1E-37	3.1E-43	9.6E-51	1.3E-59
7.5	0	0	0	8.7E-32	5.9E-32	6.3E-28	6.2E-23	4.3E-20	2.2E-19	3.2E-20	3.5E-22	3.9E-25	5.3E-29	8.5E-34	1.5E-39	1.9E-46
8.5	0	0	0	1.5E-26	2.7E-26	6.5E-23	7.1E-19	1.4E-16	5.2E-16	1.2E-16	3E-18	1.3E-20	1.0E-23	1.5E-27	3.5E-32	1.2E-37
9.5	0	0	0	5.8E-23	1.6E-22	1.5E-19	3.6E-16	3.0E-14	9.3E-14	2.8E-14	1.4E-15	1.6E-17	4.5E-20	3.1E-23	4.6E-27	1.7E-31
10.5	0	0	0	0	6.6E-20	2.9E-17	2.4E-14	1.1E-12	3.1E-12	1.2E-12	9.9E-14	2.3E-15	1.6E-17	3.6E-20	2.2E-23	5.4E-27
11.5	0	0	0	0	3.9E-18	1.1E-15	4.2E-13	1.3E-11	3.4E-11	1.6E-11	1.9E-12	7.7E-14	1.1E-15	5.5E-18	1.0E-20	1.3E-23
12.5	0	0	0	0	8.7E-17	1.4E-14	2.8E-12	6.3E-11	1.6E-10	8.8E-11	1.5E-11	9.3E-13	2.4E-14	2.3E-16	8.1E-19	0
13.5	0	0	0	0	0	7.5E-14	9.5E-12	1.7E-10	4.4E-10	2.7E-10	6.0E-11	5.4E-12	2.2E-13	3.3E-15	4.3E-17	0
14.5	0	0	0	0	0	2.6E-13	1.8E-11	3.0E-10	7.4E-10	5.3E-10	1.5E-10	1.7E-11	9.6E-13	2.4E-14	0	0
15.5	0	0	0	0	0	0	2.1E-11	3.7E-10	8.7E-10	7.6E-10	2.3E-10	3.7E-11	2.1E-12	2.2E-13	0	0
16.5	0	0	0	0	0	0	0	2.8E-10	8.2E-10	6.4E-10	3.0E-10	4.7E-11	9.6E-12	0	0	0

4.3.2 Level 2 Results for LC30

Table 20: Standard Deviation σ_{LAi} for LC30

T_z (s) → / H_S (m) ↓	3.5	4.5	5.5	6.5	7.5	8.5	9.5	10.5	11.5	12.5	13.5	14.5	15.5	16.5	17.5	18.5
0.5	0.050	0.056	0.053	0.049	0.046	0.047	0.051	0.056	0.060	0.061	0.060	0.058	0.054	0.051	0.047	0.044
1.5	0.149	0.167	0.158	0.146	0.139	0.141	0.153	0.168	0.179	0.182	0.179	0.173	0.163	0.153	0.142	0.132
2.5	0.248	0.278	0.263	0.244	0.232	0.236	0.256	0.281	0.298	0.304	0.299	0.288	0.272	0.255	0.237	0.220
3.5	0.347	0.389	0.368	0.342	0.325	0.330	0.358	0.393	0.417	0.425	0.419	0.403	0.381	0.357	0.332	0.308
4.5	0.446	0.500	0.474	0.439	0.418	0.424	0.460	0.505	0.536	0.547	0.538	0.518	0.490	0.459	0.427	0.396
5.5	0.545	0.611	0.579	0.537	0.511	0.519	0.563	0.617	0.656	0.668	0.658	0.633	0.599	0.561	0.522	0.484
6.5	0.644	0.722	0.684	0.635	0.604	0.613	0.665	0.730	0.775	0.789	0.777	0.748	0.707	0.663	0.617	0.572
7.5	0.743	0.833	0.790	0.732	0.697	0.707	0.767	0.842	0.894	0.911	0.897	0.863	0.816	0.765	0.712	0.660
8.5	0.842	0.944	0.895	0.830	0.790	0.802	0.869	0.954	1.013	1.032	1.017	0.978	0.925	0.867	0.807	0.748
9.5	0.941	1.055	1.000	0.927	0.883	0.896	0.972	1.067	1.133	1.154	1.136	1.093	1.034	0.968	0.902	0.836
10.5	1.040	1.166	1.105	1.025	0.976	0.990	1.074	1.179	1.252	1.275	1.256	1.208	1.143	1.070	0.996	0.924
11.5	1.139	1.277	1.211	1.123	1.069	1.084	1.176	1.291	1.371	1.397	1.375	1.323	1.252	1.172	1.091	1.012
12.5	1.238	1.388	1.316	1.220	1.162	1.179	1.278	1.403	1.490	1.518	1.495	1.438	1.360	1.274	1.186	1.100
13.5	1.337	1.499	1.421	1.318	1.255	1.273	1.381	1.516	1.609	1.640	1.615	1.553	1.469	1.376	1.281	1.188
14.5	1.436	1.610	1.526	1.415	1.348	1.367	1.483	1.628	1.729	1.761	1.734	1.668	1.578	1.478	1.376	1.277
15.5	1.535	1.722	1.632	1.513	1.441	1.462	1.585	1.740	1.848	1.883	1.854	1.783	1.687	1.580	1.471	1.365
16.5	1.634	1.833	1.737	1.611	1.534	1.556	1.688	1.852	1.967	2.004	1.974	1.898	1.796	1.682	1.566	1.453

Table 21: Short Term Failure Index $C_{S,i}$ for LC30

T_z (s) → / H_S (m) ↓	3.5	4.5	5.5	6.5	7.5	8.5	9.5	10.5	11.5	12.5	13.5	14.5	15.5	16.5	17.5	18.5
0.5	0	0	0	0	0	0	0	0	0	0	0	0	0	0	0	0
1.5	0	0	0	0	0	0	0	0	0	0	0	0	0	0	0	0
2.5	0	0	0	0	0	0	0	0	0	0	0	0	0	0	0	0
3.5	0	0	0	0	0	0	0	0	0	0	0	0	0	0	0	0
4.5	0	2.2E-84	7.7E-94	0	0	0	2E-99	1.3E-82	2.5E-73	1.1E-70	7.3E-73	9.4E-79	7.4E-88	0	0	0
5.5	3.5E-71	1.0E-56	4.6E-63	3.2E-73	1.2E-80	2.1E-78	9.0E-67	1.6E-55	2.5E-49	1.5E-47	5.1E-49	5.9E-53	4.7E-59	3.4E-67	2.0E-77	7.4E-90
6.5	3.6E-51	8.0E-41	2.3E-45	1.2E-52	6.1E-58	2.4E-56	5.2E-48	5.7E-40	1.6E-35	2.9E-34	2.7E-35	4.0E-38	1.7E-42	2.5E-48	1.2E-55	1.5E-64
7.5	1.3E-38	7.7E-31	3.0E-34	1.0E-39	1.1E-43	1.7E-42	3.0E-36	3.4E-30	7.3E-27	6.5E-26	1.1E-26	8.1E-29	4.3E-32	1.8E-36	5.6E-42	1.2E-48
8.5	3.2E-30	3.6E-24	8.0E-27	4.4E-31	3.5E-34	3.0E-33	2.2E-28	1.1E-23	4.5E-21	2.5E-20	6.1E-21	1.4E-22	3.8E-25	1.5E-28	7.7E-33	4.8E-38
9.5	2.4E-24	1.7E-19	1.3E-21	5.0E-25	1.6E-27	9.1E-27	7.3E-23	4.3E-19	5.1E-17	2.0E-16	6.5E-17	3.1E-18	2.8E-20	5.2E-23	2.0E-26	1.3E-30
10.5	4.7E-20	4.3E-16	7.9E-18	1.3E-20	1.2E-22	4.8E-22	7.6E-19	9.2E-16	4.6E-14	1.4E-13	5.6E-14	4.7E-15	9.9E-17	5.8E-19	9.0E-22	3.5E-25
11.5	7.7E-17	1.6E-13	5.5E-15	2.6E-17	5.3E-19	1.7E-18	7.8E-16	2.9E-13	7.6E-12	1.9E-11	9.0E-12	1.1E-12	4.6E-14	6.2E-16	2.9E-18	4.1E-21
12.5	2.3E-14	1.4E-11	8.6E-13	9.2E-15	3.4E-16	9.1E-16	1.6E-13	2.5E-11	3.9E-10	8.6E-10	4.5E-10	7.7E-11	5.1E-12	1.4E-13	1.4E-15	5.5E-18
13.5	2.0E-12	5.1E-10	4.5E-11	9.3E-13	5.4E-14	1.3E-13	1.1E-11	8.0E-10	8.6E-09	1.7E-08	9.7E-09	2.1E-09	2.1E-10	9.3E-12	1.9E-13	1.6E-15
14.5	7.3E-11	8.8E-09	1.1E-09	3.7E-11	3.2E-12	6.6E-12	3.1E-10	1.3E-08	1.0E-07	1.8E-07	1.1E-07	3.1E-08	4.1E-09	2.7E-10	9.2E-12	1.5E-13
15.5	1.3E-09	8.9E-08	1.4E-08	7.4E-10	8.7E-11	1.7E-10	4.8E-09	1.3E-07	7.6E-07	1.3E-06	8.3E-07	2.7E-07	4.5E-08	4.3E-09	2.2E-10	6.0E-12
16.5	1.5E-08	6.0E-07	1.2E-07	8.8E-09	1.3E-09	2.3E-09	4.6E-08	8.1E-07	4.0E-06	6.3E-06	4.3E-06	1.6E-06	3.3E-07	4.1E-08	3.0E-09	1.2E-10

Table 22: Long Term Failure Index Components $C_{S,i} \cdot W_i$ for LC30

T_z (s) → / H_S (m) ↓	3.5	4.5	5.5	6.5	7.5	8.5	9.5	10.5	11.5	12.5	13.5	14.5	15.5	16.5	17.5	18.5
0.5	0	0	0	0	0	0	0	0	0	0	0	0	0	0	0	0
1.5	0	0	0	0	0	0	0	0	0	0	0	0	0	0	0	0
2.5	0	0	0	0	0	0	0	0	0	0	0	0	0	0	0	0
3.5	0	0	0	0	0	0	0	0	0	0	0	0	0	0	0	0
4.5	0	0	4.6E-98	0	0	0	0	3.6E-84	3.2E-75	5.0E-73	9.6E-76	3.0E-82	5.1E-92	0	0	0
5.5	0	0	4.6E-68	1.6E-76	6.1E-83	3.3E-80	2.1E-68	3.1E-57	2.8E-51	6.8E-50	7.8E-52	2.4E-56	4.5E-63	7.0E-72	7.9E-83	7.4E-96
6.5	0	0	4.7E-51	1.6E-56	1.0E-60	1.6E-58	6.5E-50	7.3E-42	1.3E-37	1.1E-36	3.8E-38	1.7E-41	1.9E-46	6.4E-53	6.0E-61	1.5E-70
7.5	0	0	0	3.1E-44	5.5E-47	4.5E-45	1.8E-38	2.4E-32	3.8E-29	1.8E-28	1.2E-29	3.0E-32	4.4E-36	4.5E-41	3.4E-47	1.2E-54
8.5	0	0	0	3.1E-36	5.4E-38	2.9E-36	5.7E-31	4.0E-26	1.3E-23	4.3E-23	4.7E-24	3.7E-26	3.2E-29	3.2E-33	3.8E-38	4.8E-44
9.5	0	0	0	1.0E-30	7.1E-32	3.0E-30	7.4E-26	6.8E-22	7.8E-20	2.0E-19	3.2E-20	5.8E-22	1.7E-24	8.9E-28	7.8E-32	1.3E-36
10.5	0	0	0	0	1.4E-27	5.2E-26	2.9E-22	6.2E-19	3.3E-17	7.3E-17	1.5E-17	5.3E-19	4.0E-21	6.9E-24	2.7E-27	3.5E-31
11.5	0	0	0	0	1.6E-24	5.6E-23	1E-19	7.7E-17	2.4E-15	4.8E-15	1.3E-15	7.2E-17	1.1E-18	4.4E-21	5.7E-24	4.1E-27
12.5	0	0	0	0	3.4E-22	9.1E-21	7.2E-18	2.4E-15	5.0E-14	9.4E-14	3.0E-14	2.5E-15	6.6E-17	5.4E-19	1.4E-21	0
13.5	0	0	0	0	0	3.8E-19	1.5E-16	2.8E-14	4.3E-13	7.7E-13	3.0E-13	3.4E-14	1.5E-15	1.9E-17	1.9E-19	0
14.5	0	0	0	0	0	6.6E-18	1.3E-15	1.6E-13	1.8E-12	3.3E-12	1.5E-12	2.1E-13	1.2E-14	2.7E-16	0	0
15.5	0	0	0	0	0	0	4.8E-15	5.0E-13	4.6E-12	8.9E-12	4.2E-12	8.0E-13	4.5E-14	4.3E-15	0	0
16.5	0	0	0	0	0	0	0	8.1E-13	8.0E-12	1.3E-11	8.6E-12	1.6E-12	3.3E-13	0	0	0

4.3.3 Level 2 Results for LC36

Table 23: Standard Deviation σ_{LAi} for LC36

T_z (s) → / H_S (m) ↓	3.5	4.5	5.5	6.5	7.5	8.5	9.5	10.5	11.5	12.5	13.5	14.5	15.5	16.5	17.5	18.5
0.5	0.097	0.093	0.084	0.078	0.079	0.088	0.097	0.100	0.098	0.093	0.087	0.080	0.073	0.067	0.061	0.056
1.5	0.292	0.279	0.251	0.233	0.238	0.265	0.290	0.300	0.295	0.280	0.261	0.240	0.220	0.201	0.183	0.167
2.5	0.487	0.466	0.419	0.389	0.397	0.442	0.484	0.500	0.491	0.467	0.435	0.400	0.366	0.334	0.305	0.278
3.5	0.682	0.652	0.586	0.545	0.556	0.619	0.677	0.700	0.688	0.654	0.609	0.561	0.513	0.468	0.427	0.390
4.5	0.877	0.838	0.754	0.700	0.715	0.795	0.871	0.900	0.885	0.841	0.783	0.721	0.660	0.602	0.549	0.501
5.5	1.072	1.024	0.922	0.856	0.874	0.972	1.065	1.100	1.081	1.028	0.957	0.881	0.806	0.736	0.671	0.613
6.5	1.267	1.211	1.089	1.012	1.033	1.149	1.258	1.300	1.278	1.214	1.131	1.041	0.953	0.869	0.793	0.724
7.5	1.462	1.397	1.257	1.167	1.192	1.326	1.452	1.500	1.474	1.401	1.305	1.201	1.099	1.003	0.915	0.835
8.5	1.656	1.583	1.424	1.323	1.351	1.502	1.645	1.700	1.671	1.588	1.479	1.361	1.246	1.137	1.037	0.947
9.5	1.851	1.769	1.592	1.479	1.510	1.679	1.839	1.900	1.867	1.775	1.653	1.522	1.392	1.271	1.159	1.058
10.5	2.046	1.956	1.759	1.634	1.669	1.856	2.032	2.100	2.064	1.962	1.827	1.682	1.539	1.404	1.281	1.169
11.5	2.241	2.142	1.927	1.790	1.828	2.033	2.226	2.300	2.261	2.149	2.001	1.842	1.685	1.538	1.403	1.281
12.5	2.436	2.328	2.094	1.945	1.987	2.209	2.419	2.500	2.457	2.335	2.175	2.002	1.832	1.672	1.525	1.392
13.5	2.631	2.514	2.262	2.101	2.146	2.386	2.613	2.700	2.654	2.522	2.349	2.162	1.979	1.806	1.647	1.503
14.5	2.826	2.701	2.429	2.257	2.305	2.563	2.806	2.900	2.850	2.709	2.523	2.323	2.125	1.939	1.769	1.615
15.5	3.020	2.887	2.597	2.412	2.464	2.740	3.000	3.100	3.047	2.896	2.697	2.483	2.272	2.073	1.891	1.726
16.5	3.215	3.073	2.765	2.568	2.623	2.916	3.194	3.300	3.243	3.083	2.871	2.643	2.418	2.207	2.013	1.838

Table 24: Short Term Failure Index $C_{S,i}$ for LC36

T_z (s) → / H_S (m) ↓	3.5	4.5	5.5	6.5	7.5	8.5	9.5	10.5	11.5	12.5	13.5	14.5	15.5	16.5	17.5	18.5
0.5	0	0	0	0	0	0	0	0	0	0	0	0	0	0	0	0
1.5	0	0	0	0	0	0	0	0	0	0	0	0	0	0	0	0
2.5	8.9E-89	4.2E-97	0	0	0	0	5.6E-90	2.6E-84	2.9E-87	1.6E-96	0	0	0	0	0	0
3.5	1.2E-45	6.7E-50	1.7E-61	3.7E-71	3.0E-68	2.5E-55	2.9E-46	2.3E-43	7.1E-45	1.3E-49	4.5E-57	3.2E-67	3.8E-80	4.3E-96	0	0
4.5	6.7E-28	1.8E-30	1.7E-37	2.5E-43	1.4E-41	9.2E-34	2.8E-28	1.6E-26	2.0E-27	2.7E-30	8.2E-35	6.0E-41	9.0E-49	2.0E-58	4.6E-70	6.3E-84
5.5	6.4E-19	1.2E-20	2.5E-25	3.0E-29	4.5E-28	7.7E-23	3.6E-19	5.4E-18	1.3E-18	1.6E-20	1.5E-23	1.2E-27	6.9E-33	2.4E-39	3.8E-47	2.0E-56
6.5	9.4E-14	5.5E-15	2.4E-18	3.8E-21	2.6E-20	1.5E-16	6.3E-14	4.3E-13	1.6E-13	6.8E-15	4.6E-17	5.3E-20	9.4E-24	2.2E-28	5.8E-34	1.3E-40
7.5	1.6E-10	2.0E-11	5.8E-14	4.6E-16	2.0E-15	1.3E-12	1.2E-10	5.2E-10	2.4E-10	2.3E-11	5.4E-13	3.3E-15	5.1E-18	1.7E-21	1.1E-25	1.1E-30
8.5	2.4E-08	4.6E-09	5.0E-11	1.1E-12	3.6E-12	5.5E-10	1.9E-08	5.9E-08	3.3E-08	5.2E-09	2.8E-10	5.3E-12	3.4E-14	6.8E-17	3.7E-20	4.8E-24
9.5	8.0E-07	2.1E-07	5.6E-09	2.8E-10	6.8E-10	3.9E-08	6.6E-07	1.6E-06	1.0E-06	2.3E-07	2.2E-08	9.4E-10	1.7E-11	1.1E-13	2.8E-16	2.1E-19
10.5	1.0E-05	3.4E-06	1.8E-07	1.5E-08	3.1E-08	8.6E-07	8.7E-06	1.8E-05	1.2E-05	3.7E-06	5.5E-07	4.1E-08	1.5E-09	2.5E-11	1.8E-13	5.2E-16
11.5	6.9E-05	2.8E-05	2.4E-06	3.0E-07	5.6E-07	8.7E-06	6.1E-05	1.1E-04	8.1E-05	3.0E-05	6.0E-06	6.9E-07	4.4E-08	1.5E-09	2.4E-11	1.8E-13
12.5	3.0E-04	1.4E-04	1.7E-05	3.0E-06	5.1E-06	5.2E-05	2.7E-04	4.5E-04	3.5E-04	1.5E-04	3.8E-05	6.1E-06	5.9E-07	3.3E-08	1.0E-09	1.6E-11
13.5	9.6E-04	5.0E-04	8.2E-05	1.8E-05	2.9E-05	2.1E-04	8.7E-04	1.4E-03	1.1E-03	5.2E-04	1.6E-04	3.4E-05	4.6E-06	3.9E-07	2.0E-08	5.7E-10
14.5	2.4E-03	1.4E-03	2.9E-04	7.9E-05	1.2E-04	6.6E-04	2.2E-03	3.3E-03	2.7E-03	1.4E-03	5.2E-04	1.3E-04	2.4E-05	2.8E-06	2.1E-07	9.7E-09
15.5	5.1E-03	3.1E-03	8.0E-04	2.6E-04	3.6E-04	1.6E-03	4.8E-03	6.7E-03	5.6E-03	3.2E-03	1.3E-03	4.1E-04	8.9E-05	1.4E-05	1.4E-06	9.7E-08
16.5	9.5E-03	6.1E-03	1.8E-03	6.8E-04	9.2E-04	3.5E-03	8.9E-03	1.2E-02	1.0E-02	6.3E-03	2.9E-03	1.0E-03	2.7E-04	5.1E-05	7.0E-06	6.5E-07

Table 25: Long Term Failure Index Components $C_{S,i} \cdot W_i$ for LC36

T_z (s) → / H_S (m) ↓	3.5	4.5	5.5	6.5	7.5	8.5	9.5	10.5	11.5	12.5	13.5	14.5	15.5	16.5	17.5	18.5
0.5	0	0	0	0	0	0	0	0	0	0	0	0	0	0	0	0
1.5	0	0	0	0	0	0	0	0	0	0	0	0	0	0	0	0
2.5	0	0	0	0	0	0	2.7E-91	5.4E-86	1.9E-89	3E-99	0	0	0	0	0	0
3.5	0	1.3E-55	6.0E-65	2.6E-73	9.7E-70	1.4E-56	1.5E-47	6.4E-45	7.9E-47	4.6E-52	3.8E-60	5.9E-71	1.3E-84	0	0	0
4.5	0	0	1.0E-41	4.9E-46	1.9E-43	3.0E-35	1.1E-29	4.3E-28	2.5E-29	1.2E-32	1.1E-37	1.9E-44	6.2E-53	2.6E-63	9.1E-76	0
5.5	0	0	2.5E-30	1.5E-32	2.3E-30	1.2E-24	8.6E-21	1.1E-19	1.5E-20	7.5E-23	2.3E-26	4.9E-31	6.7E-37	5.0E-44	1.5E-52	2.0E-62
6.5	0	0	4.8E-24	4.8E-25	4.4E-23	1.0E-18	7.9E-16	5.5E-15	1.3E-15	2.6E-17	6.5E-20	2.2E-23	1.0E-27	5.6E-33	2.9E-39	1.3E-46
7.5	0	0	0	1.4E-20	1.0E-18	3.5E-15	7.2E-13	3.6E-12	1.3E-12	6.3E-14	6.0E-16	1.2E-18	5.2E-22	4.3E-26	6.5E-31	1.1E-36
8.5	0	0	0	8.0E-18	5.5E-16	5.4E-13	4.9E-11	2.1E-10	9.7E-11	9.0E-12	2.2E-13	1.5E-15	2.9E-18	1.5E-21	1.8E-25	4.8E-30
9.5	0	0	0	5.5E-16	2.9E-14	1.3E-11	6.7E-10	2.6E-09	1.5E-09	2.3E-10	1.1E-11	1.8E-13	1.0E-15	1.9E-18	1.1E-21	2.1E-25
10.5	0	0	0	0	3.8E-13	9.2E-11	3.3E-09	1.2E-08	8.9E-09	1.9E-09	1.5E-10	4.7E-12	6.0E-14	3.0E-16	5.5E-19	5.2E-22
11.5	0	0	0	0	1.7E-12	2.9E-10	8.1E-09	3.0E-08	2.6E-08	7.3E-09	8.6E-10	4.4E-11	1.1E-12	1.0E-14	4.8E-17	1.8E-19
12.5	0	0	0	0	5.1E-12	5.2E-10	1.2E-08	4.5E-08	4.4E-08	1.6E-08	2.6E-09	2.0E-10	7.7E-12	1.3E-13	1.0E-15	0
13.5	0	0	0	0	0	6.4E-10	1.2E-08	4.8E-08	5.4E-08	2.4E-08	5.1E-09	5.4E-10	3.2E-11	7.8E-13	2.0E-14	0
14.5	0	0	0	0	0	6.6E-10	8.9E-09	3.9E-08	4.8E-08	2.6E-08	6.8E-09	9.4E-10	7.1E-11	2.8E-12	0	0
15.5	0	0	0	0	0	0	4.8E-09	2.7E-08	3.4E-08	2.3E-08	6.7E-09	1.2E-09	8.9E-11	1.4E-11	0	0
16.5	0	0	0	0	0	0	0	1.2E-08	2.1E-08	1.3E-08	5.8E-09	1.0E-09	2.7E-10	0	0	0

4.3.4 Level 2 Results for LC39

Table 26: Standard Deviation σ_{LAi} for LC39

T_z (s) → / H_S (m) ↓	3.5	4.5	5.5	6.5	7.5	8.5	9.5	10.5	11.5	12.5	13.5	14.5	15.5	16.5	17.5	18.5
0.5	0.134	0.121	0.108	0.104	0.113	0.127	0.133	0.130	0.123	0.113	0.103	0.094	0.085	0.076	0.069	0.063
1.5	0.403	0.364	0.324	0.311	0.340	0.380	0.398	0.391	0.369	0.340	0.310	0.281	0.254	0.229	0.208	0.188
2.5	0.671	0.607	0.539	0.518	0.567	0.633	0.663	0.652	0.615	0.567	0.517	0.468	0.423	0.382	0.346	0.314
3.5	0.939	0.849	0.755	0.726	0.794	0.887	0.928	0.912	0.861	0.794	0.723	0.655	0.592	0.535	0.484	0.439
4.5	1.208	1.092	0.971	0.933	1.020	1.140	1.193	1.173	1.107	1.021	0.930	0.842	0.761	0.688	0.623	0.565
5.5	1.476	1.334	1.187	1.140	1.247	1.393	1.458	1.434	1.353	1.248	1.136	1.029	0.930	0.840	0.761	0.691
6.5	1.745	1.577	1.403	1.347	1.474	1.647	1.724	1.695	1.600	1.475	1.343	1.216	1.099	0.993	0.899	0.816
7.5	2.013	1.820	1.618	1.555	1.701	1.900	1.989	1.955	1.846	1.702	1.550	1.403	1.268	1.146	1.038	0.942
8.5	2.282	2.062	1.834	1.762	1.927	2.154	2.254	2.216	2.092	1.929	1.756	1.590	1.437	1.299	1.176	1.067
9.5	2.550	2.305	2.050	1.969	2.154	2.407	2.519	2.477	2.338	2.156	1.963	1.777	1.606	1.451	1.314	1.193
10.5	2.818	2.547	2.266	2.177	2.381	2.660	2.784	2.737	2.584	2.382	2.169	1.964	1.775	1.604	1.453	1.318
11.5	3.087	2.790	2.482	2.384	2.608	2.914	3.050	2.998	2.830	2.609	2.376	2.151	1.944	1.757	1.591	1.444
12.5	3.355	3.033	2.697	2.591	2.834	3.167	3.315	3.259	3.076	2.836	2.583	2.338	2.113	1.910	1.729	1.570
13.5	3.624	3.275	2.913	2.799	3.061	3.420	3.580	3.519	3.322	3.063	2.789	2.525	2.282	2.063	1.868	1.695
14.5	3.892	3.518	3.129	3.006	3.288	3.674	3.845	3.780	3.568	3.290	2.996	2.712	2.451	2.215	2.006	1.821
15.5	4.161	3.761	3.345	3.213	3.515	3.927	4.110	4.041	3.814	3.517	3.203	2.899	2.620	2.368	2.144	1.946
16.5	4.429	4.003	3.561	3.420	3.741	4.180	4.375	4.302	4.060	3.744	3.409	3.086	2.789	2.521	2.283	2.072

Table 27: Short Term Failure Index $C_{S,i}$ for LC39

T_z (s) → / H_S (m) ↓	3.5	4.5	5.5	6.5	7.5	8.5	9.5	10.5	11.5	12.5	13.5	14.5	15.5	16.5	17.5	18.5
0.5	0	0	0	0	0	0	0	0	0	0	0	0	0	0	0	0
1.5	0	0	0	0	0	0	0	0	0	0	0	0	0	0	0	0
2.5	3.9E-47	1.6E-57	1.6E-72	1.6E-78	9.3E-66	8.2E-53	2.8E-48	6.4E-50	6.1E-56	1.1E-65	4.8E-79	2.8E-96	0	0	0	0
3.5	2.1E-24	1.0E-29	2.3E-37	2.0E-40	6.6E-34	2.7E-27	5.5E-25	7.9E-26	6.7E-29	7.3E-34	1.1E-40	1.8E-49	1.9E-60	8.3E-74	7.3E-90	0
4.5	4.8E-15	2.9E-18	6.9E-23	9.7E-25	8.5E-21	8.4E-17	2.1E-15	6.5E-16	9.1E-18	9.0E-21	6.7E-25	3.2E-30	7.5E-37	6.2E-45	1.2E-54	3.5E-66
5.5	2.6E-10	1.8E-12	1.5E-15	8.4E-17	3.7E-14	1.7E-11	1.5E-10	6.8E-11	3.9E-12	3.8E-14	6.6E-17	1.8E-20	6.6E-25	2.5E-30	8.0E-37	1.5E-44
6.5	1.4E-07	4.0E-09	2.4E-11	3.1E-12	2.4E-10	2.0E-08	9.3E-08	5.3E-08	6.8E-09	2.5E-10	2.6E-12	7.3E-15	4.9E-18	6.5E-22	1.4E-26	4.3E-32
7.5	7.0E-06	4.9E-07	1.1E-08	2.3E-09	5.9E-08	1.6E-06	5.2E-06	3.4E-06	7.3E-07	6.1E-08	2.0E-09	2.4E-11	9.9E-14	1.2E-16	3.9E-20	2.7E-24
8.5	9.7E-05	1.2E-05	6.1E-07	1.9E-07	2.4E-06	3.1E-05	7.7E-05	5.5E-05	1.7E-05	2.4E-06	1.7E-07	5.4E-09	7.5E-11	4.1E-13	7.7E-16	4.5E-19
9.5	6.1E-04	1.2E-04	1.1E-05	4.1E-06	3.1E-05	2.5E-04	5.1E-04	3.9E-04	1.5E-04	3.2E-05	3.8E-06	2.4E-07	7.8E-09	1.2E-10	8.0E-13	2.1E-15
10.5	2.3E-03	6.0E-04	8.5E-05	3.9E-05	2.1E-04	1.1E-03	2.0E-03	1.6E-03	7.4E-04	2.1E-04	3.6E-05	3.8E-06	2.3E-07	7.6E-09	1.2E-10	9.5E-13
11.5	6.4E-03	2.1E-03	4.0E-04	2.1E-04	8.4E-04	3.5E-03	5.7E-03	4.7E-03	2.5E-03	8.5E-04	2.0E-04	3.0E-05	2.9E-06	1.7E-07	5.5E-09	9.5E-11
12.5	1.4E-02	5.3E-03	1.3E-03	7.7E-04	2.5E-03	8.3E-03	1.3E-02	1.1E-02	6.2E-03	2.5E-03	7.4E-04	1.5E-04	2.1E-05	1.9E-06	1.0E-07	3.3E-09
13.5	2.6E-02	1.1E-02	3.4E-03	2.1E-03	5.9E-03	1.6E-02	2.3E-02	2.1E-02	1.3E-02	5.9E-03	2.1E-03	5.3E-04	9.7E-05	1.2E-05	1.0E-06	5.3E-08
14.5	4.2E-02	2.0E-02	7.3E-03	4.9E-03	1.2E-02	2.8E-02	3.9E-02	3.4E-02	2.3E-02	1.2E-02	4.7E-03	1.4E-03	3.3E-04	5.5E-05	6.4E-06	5.0E-07
15.5	6.2E-02	3.3E-02	1.4E-02	9.5E-03	2.0E-02	4.4E-02	5.8E-02	5.3E-02	3.7E-02	2.0E-02	9.2E-03	3.3E-03	9.0E-04	1.9E-04	2.9E-05	3.0E-06
16.5	8.6E-02	5.0E-02	2.2E-02	1.6E-02	3.2E-02	6.4E-02	8.1E-02	7.4E-02	5.4E-02	3.2E-02	1.6E-02	6.4E-03	2.1E-03	5.1E-04	9.8E-05	1.4E-05

Table 28: Long Term Failure Index Components $C_{S,i} \cdot W_i$ for LC39

T_z (s) → / H_S (m) ↓	3.5	4.5	5.5	6.5	7.5	8.5	9.5	10.5	11.5	12.5	13.5	14.5	15.5	16.5	17.5	18.5
0.5	0	0	0	0	0	0	0	0	0	0	0	0	0	0	0	0
1.5	0	0	0	0	0	0	0	0	0	0	0	0	0	0	0	0
2.5	0	3.5E-62	3.1E-75	3.4E-80	5.8E-67	6.1E-54	1.4E-49	1.3E-51	3.9E-58	1.8E-68	1.6E-82	2E-100	0	0	0	0
3.5	0	2.1E-35	8.1E-41	1.4E-42	2.1E-35	1.5E-28	2.8E-26	2.3E-27	7.5E-31	2.5E-36	9.3E-44	3.2E-53	6.8E-65	5E-79	7.3E-96	0
4.5	0	0	4.1E-27	1.9E-27	1.1E-22	2.8E-18	8.1E-17	1.8E-17	1.2E-19	4.1E-23	8.8E-28	1.0E-33	5.2E-41	8.0E-50	2.4E-60	0
5.5	0	0	1.5E-20	4.3E-20	1.8E-16	2.8E-13	3.6E-12	1.4E-12	4.4E-14	1.8E-16	9.9E-20	7.4E-24	6.4E-29	5.3E-35	3.2E-42	1.5E-50
6.5	0	0	4.8E-17	3.9E-16	4.0E-13	1.4E-10	1.2E-09	6.7E-10	5.6E-11	9.5E-13	3.7E-15	3.1E-18	5.3E-22	1.6E-26	7.1E-32	4.3E-38
7.5	0	0	0	6.8E-14	3.1E-11	4.4E-09	3.1E-08	2.4E-08	3.8E-09	1.7E-10	2.2E-12	8.9E-15	1.0E-17	3.0E-21	2.3E-25	2.7E-30
8.5	0	0	0	1.3E-12	3.6E-10	3.1E-08	2.0E-07	1.9E-07	5.0E-08	4.2E-09	1.3E-10	1.5E-12	6.3E-15	8.9E-18	3.8E-21	4.5E-25
9.5	0	0	0	8.2E-12	1.3E-09	8.2E-08	5.2E-07	6.3E-07	2.3E-07	3.2E-08	1.8E-09	4.5E-11	4.8E-13	2.0E-15	3.2E-18	2.1E-21
10.5	0	0	0	0	2.5E-09	1.2E-07	7.6E-07	1.1E-06	5.3E-07	1.1E-07	9.9E-09	4.4E-10	9.3E-12	9.1E-14	3.7E-16	9.5E-19
11.5	0	0	0	0	2.5E-09	1.1E-07	7.5E-07	1.3E-06	7.7E-07	2.1E-07	2.8E-08	2.0E-09	7.1E-11	1.2E-12	1.1E-14	9.5E-17
12.5	0	0	0	0	2.5E-09	8.3E-08	5.5E-07	1.1E-06	7.9E-07	2.8E-07	5.0E-08	5.0E-09	2.7E-10	7.5E-12	1.0E-13	0
13.5	0	0	0	0	0	4.9E-08	3.3E-07	7.2E-07	6.4E-07	2.7E-07	6.4E-08	8.5E-09	6.8E-10	2.4E-11	1.0E-12	0
14.5	0	0	0	0	0	2.8E-08	1.5E-07	4.1E-07	4.1E-07	2.1E-07	6.1E-08	1.0E-08	1.0E-09	5.5E-11	0	0
15.5	0	0	0	0	0	0	5.8E-08	2.1E-07	2.2E-07	1.4E-07	4.6E-08	9.8E-09	9.0E-10	1.9E-10	0	0
16.5	0	0	0	0	0	0	0	7.4E-08	1.1E-07	6.5E-08	3.2E-08	6.4E-09	2.1E-09	0	0	0

4.3.5 Collective Level 2 Results

By adding all the elements from the Tables 19, 22, 25 and 28, you get the long-term failure index C for each loading condition. If the sum is equal or lower to the predefined threshold of the criterion R_{EA2} = 0.00039, then the ship in that loading condition is considered as not vulnerable to excessive acceleration. The results are shown in Table 29:

Table 29: Level 2 EA Results

Loading Conditions	LC21	LC30	LC36	LC39
Long Term Probability Index, C	7.502E-9	5.947E-11	6.471E-07	1.498E-05
Status	**Pass**	**Pass**	**Pass**	**Pass**

It's easily noticeable that the ship passes the Level 2 criterion, for all four loading conditions, as it was expected, given the fact that Level 1 passed. That means that no inconsistency errors appear in this specific model ship, for the four loading conditions that were chosen.

4.4 CSM Application

One of the main differences between the EA and CSM criteria, is that their application is made in different places on the ship. As explained earlier, the EA criterion is applied on the bridge deck, being the most hazardous place for the crew members, in regards of lateral acceleration. The CSM has to be applied for all the container stacks using lashings on the deck of the ship. Therefore, the places of the containers have to be determined. For a better view of the criterion, the calculations are going to be made in three different places, along the ship deck and for two loading conditions LC36 and LC39. Only the results for the particulars that affect the final lashing forces are going to be presented, the rest where only mentioned in Chapter 3, for a complete description of the CSM calculations.

4.4.1 Container and Lashing Data

According to the international standards, and more specifically ISO 668 the typical dimensions of a 20 ft container are shown in Table 30 [25]:

Table 30: 20 ft Container Dimensions

Dimensions	Symbol	Value (m)
Length	L_C	6.058
Width	W_C	2.438
Height	H_C	2.591

As stated before, the calculations for the forces acting on the lashings, are going to be made in stacks of three containers for one and two pair of lashings, in three different positions aboard the ship. The choices for the stack positions are shown in meters, in Table 31 (longitudinal from AP and transverse from midship):

Table 31: Container Positions

Distance	Symbol	Stack No		
		1	2	3
Longitudinal	x_C (m)	13.88	106.98	213.71
Transverse	y_C (m)	0	17.432	0

The calculations are performed three times with the stack being placed near the stern, midship and bow, respectively. The vertical distance z_C from the BL of each container for all three stacks is:

$$z_C = \begin{cases} 20.9 \text{ m}, & \text{for the bottom container} \\ 23.5 \text{ m}, & \text{for the middle container} \\ 26.1 \text{ m}, & \text{for the top container} \end{cases}$$

For the lashings the index 1 denotes the lashing crossing only the bottom container and the index 2 the lashing crossing the bottom and middle containers (when present). In order to estimate the cross section of the lashing, its diameter is needed. It was taken equal to 24 mm, same as past works in a similar subject. All the needed information for the lashings is in Table 32:

Table 32: Lashing Data

Particulars	Values
L_y (mm)	2438
L_{z1} (mm)	2591
L_{z2} (mm)	5182
L_{l1} (mm)	3557.7
L_{l2} (mm)	5726.9
A_l (mm^2)	452.39
E_{l1} (GPa)	97.1
E_{l2} (GPa)	176.6
K_{l1} (kN/mm)	12.35
K_{l2} (kN/mm)	13.95
β_1 (rad)	0.816
β_2 (rad)	1.131
K_{lh1} (kN/mm)	5.80
K_{lh2} (kN/mm)	2.53

4.4.2 Initial Calculations

Firstly, the results for the natural roll period, T_r, and the roll amplitude, φ and height of the roll center, R_{CTR}, are shown in Table 33:

Table 33: Initial Calculations for CSM

Particulars	Loading Conditions			
	21	30	36	39
T_r (s)	19.42	20.84	17.68	16.14
φ (rad)	0.367	0.367	0.383	0.441
φ (deg)	21.04	21.04	21.95	25.25
R_{CTR} (m)	11.16	10.66	10.66	10.66

The method for calculating these quantities is way different than the method used by IMO Guidelines so values obviously, are going to differ greatly.

4.4.3 Accelerations

In the next Tables, the common acceleration a_0, the transverse static gravitational acceleration component a_{GT}, the transverse roll acceleration component a_{RT} and the lateral acceleration A_T, for Condition A are presented (being the only accelerations affecting the lashing forces, as explained in Chapter 3), for the three container positions and the two chosen loading conditions. The first three accelerations don't take into account the position of the stack, so it's the same value for all 3 container positions. The numbers inside the bracket denote the three containers of the stack starting with the bottom one. Their values in m/s^2 are shown in Table 34:

Table 34: CSM Accelerations

Accelerations	Loading Conditions					
	36			39		
	Stack No					
	1	2	3	1	2	3
k_3	0.3544	0	0.4588	0.3544	0	0.4588
a_0 (m/s^2)	1.28			1.34		
a_{GT} (m/s^2)	3.67			4.18		
a_{RT} (m/s^2)	{7.05, 8.34, 10.62}			{9.74, 12.20, 14.67}		
A_T (m/s^2)	{4.81, 4.93, 5.06}	{4.64, 4.76, 4.89}	{4.86, 4.98, 5.11}	{5.64, 5.82, 5.98}	{5.44, 5.61, 5.78}	{5.70, 5.88, 6.05}

4.4.4 Container and Lashing Forces

The wind force acting of the sides of the container for all the containers in any loading condition, as its value is only depending on the container's dimensions, is:

$$F_W = 8.48\ \text{kN}$$

Knowing the transverse acceleration, the horizontal force, F_H, in every container can be calculated. For the weight of each container, giving the lack of more information, the homogenous weight of every loading condition (16 t for LC36 and 18 t for LC39) is going to be utilized. So, the horizontal force of all three containers, in every stack is shown in Table 35, in kN:

Table 35: Horizontal Force F_H for every Container

Stack	LC36			LC39		
	Bottom	Middle	Top	Bottom	Middle	Top
1	39.57	40.08	40.59	50.78	52.34	53.89
2	37.11	38.11	39.12	48.96	50.51	52.06
3	38.87	39.87	40.87	51.32	52.88	54.43

Now similarly, the racking force Q_i acting at the top of each container is shown in Table 36 in kN:

Table 36: Racking force Q_i for every Container

Stack	LC36			LC39		
	Bottom	Middle	Top	Bottom	Middle	Top
1	118.45	70.95	22.45	150.27	90.16	28.49
2	115.13	68.98	21.84	145.80	87.51	27.66
3	119.43	71.53	22.63	151.59	90.94	28.73

So, finally, the horizontal force component of the lashing, F_{lH}, and the lashing tension, T_l, for both of the lashing arrangements (single lash and double lash to deck), are shown in Table 37, in kN:

Table 37: Lashing Loads

Arrangement	Force	Loading Conditions					
		36			39		
		Stack No					
		1	2	3	1	2	3
Single lash	F_{lh1} (kN)	72.08	70.06	72.67	91.45	88.72	92.25
	T_{l1} (kN)	105.18	102.23	106.05	133.44	129.47	134.62
Double lash	F_{lh1} (kN)	47.18	45.85	47.57	59.82	58.03	60.35
	T_{l1} (kN)	68.84	66.90	69.41	87.29	84.68	88.06
	F_{lh2} (kN)	40.92	39.78	41.26	51.97	50.43	52.42
	T_{l2} (kN)	96.13	93.45	96.92	122.08	118.47	123.14

With a quick check at Table 37, it's obvious that no lash tension surpasses the Calculated Strength of 195.33 kN, meaning that the lashings are in no danger of breaking at any point of the trip and the system is secured.

Chapter 5: Discussion of the Results

From the Tables in Chapter 4 it's apparent that the model ship satisfies all three criteria, for all the chosen loading conditions. Therefore, more analysis is needed in order to make an adequate judgement on which criterion is stricter. The results are firstly, going to be compared to each other and then the same calculations are going to be conducted with some of the parameters changed. This way it will be easy to figure out which criterion fails first and also how much does each parameter affects the final result. Additionally, the analysis explores whether the application of either the CSM or the EA criterion, can be omitted, while still satisfying both criteria.

5.1 Level 1 EA Criterion Results

Taking a look at the results of Table 13 and the characteristics of Table 9, there's a clear connection between the GM and the values of the characteristic roll amplitude and lateral acceleration, as anticipated. Loading conditions with higher metacentric height, seem to result in quicker roll oscillations (smaller natural roll period) and larger roll angles, meaning higher accelerations are achieved and the criterion is more probable to fail. The same can be said for the vertical distance of the bridge deck from the roll axis, h_r, or similarly for the center of gravity, KG. The higher h_r (or lower KG), results in higher final values of the criterion.

Now, in order to determine the sensitivity of certain parameters and which one affects the final result the most, they will be altered individually while all other values remain constant until the criterion fails. For reasons of simplicity, it is assumed that by changing one parameter, all the others remain constant. The changes, however, must be within reasonable values to ensure the results are somewhat realistic. For the calculations, the loading condition 36 was used, for all the parameters except the one being changed. The three parameters to be altered are the GM, the height of the bridge deck from the Baseline, h_k, and the KG. The results are presented below in the form of matrices and graphs.

5.1.1 Connection of Metacentric Height with Lateral Acceleration

The calculations were performed again for GM values from 1 to 10 m, with an interval of 1 m. It is known, from past incidents, that when a ship with similar dimensions, develops a metacentric height of around 5 meters or more, due to the action of waves, acceleration problems can occur. The results for the roll angle, in degrees and rad, and the acceleration are shown in Table 38 and Figure 15 and 16. In Figure 16, the upper limit of the criterion (4.64 m/s^2), is shown as the red horizontal line.

Table 38: GM – φ and a_y

GM (m)	φ (rad)	φ (deg)	a_y (m/s^2)	Status
2	0.177	10.12	2.46	**Pass**
3	0.217	12.42	3.45	**Pass**
4	0.246	14.10	4.41	**Pass**
5	0.262	15.03	5.22	**Fail**
6	0.269	15.41	5.88	**Fail**
7	0.268	15.35	6.39	**Fail**
8	0.262	15.03	6.78	**Fail**
9	0.254	14.55	7.06	**Fail**
10	0.244	13.98	7.27	**Fail**

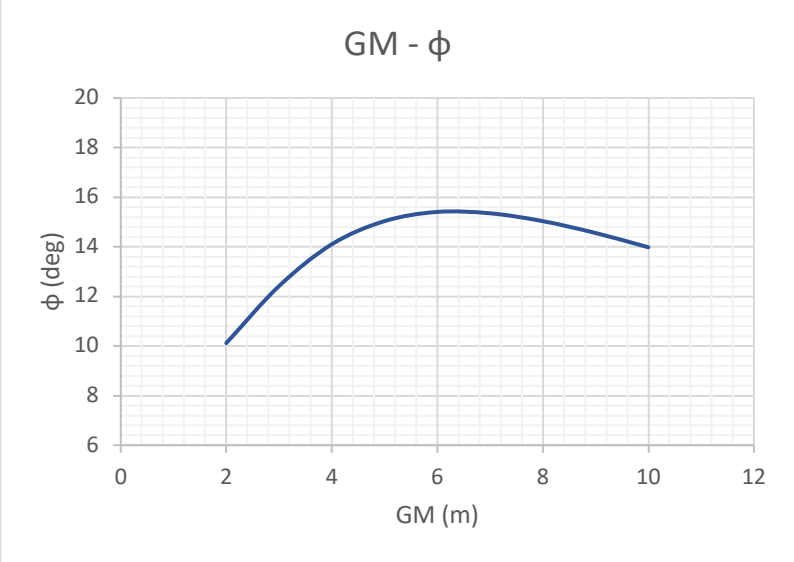

Figure 13: GM – φ

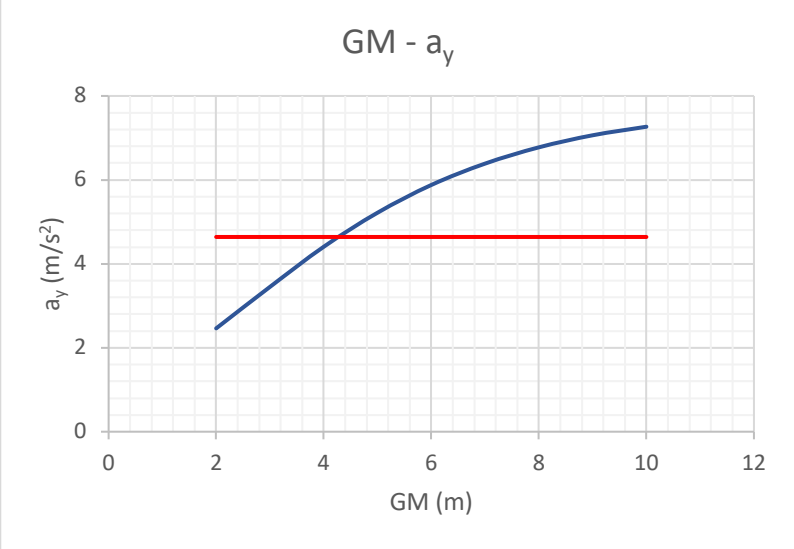

Figure 14: GM – a_y

Looking at the Tables and Figures above, it seems that the critical GM point is around 4.3 m. That means, with an increase of 50% from the initial GM value, the Level 1 criterion fails. For GM values larger than that, the Level 2 has to be performed, as well, in order to characterize the ship as vulnerable or not, to excessive acceleration. The relation between the GM and the acceleration is easily noticeable. The continuous increase of GM, results in quicker accelerations, as expected. This effect, however, seems to reduce in higher values and tends to obtain a specific value.

The same can't be said for the relation between GM and the roll angle. In lower GM values the amplitude gets bigger but after 6 m the amplitude seems to start dropping. There are many reasons that this can be explained. One of which is that there is no clear connection between those two values, in general. Smaller metacentric heights don't always result in smaller rolling angles. It can also, be addressed to the errors in the method, since, realistically other particulars change as well with the increase of GM.

5.1.2 Connection of Height with Lateral Acceleration

The height of the bridge deck from the Baseline, h_k, is taken from 40 to 90 m with a 5 m interval. From the analysis of the criterion, it shows that it doesn't affect the roll amplitude but only the lateral acceleration. So, their relation is shown in Table 39 and Figure 17:

Table 39: GM – h_k

h_k (m)	h_r (m)	a_y (m/s^2)	Status
40	26.83	3.12	**Pass**
45	31.83	3.30	**Pass**
50	36.83	3.49	**Pass**
55	41.83	3.68	**Pass**
60	46.83	3.87	**Pass**
65	51.83	4.05	**Pass**
70	56.83	4.24	**Pass**
75	61.83	4.43	**Pass**
80	66.83	4.62	**Pass**
85	71.83	4.80	**Fail**
90	76.83	4.99	**Fail**

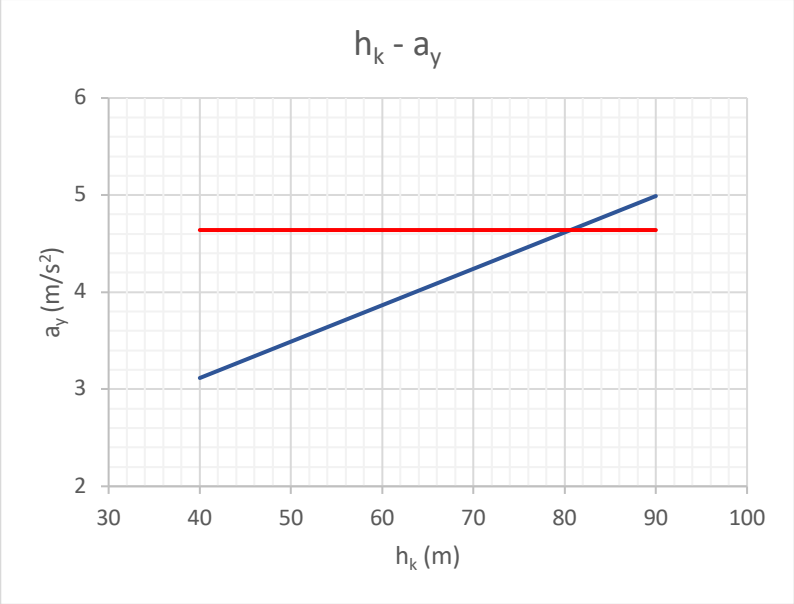

Figure 15: h_k – a_y

The connection between these two particulars is obviously linear. However, the vertical distance has to be almost doubled and become unreasonably large, for the criterion to fail. Having a bridge deck that high will also cause stability problems due to higher wind forces. So, it's clear that the height of the bridge deck doesn't affect the final result as much as the metacentric height does.

5.1.3 Connection of Center of Gravity with Lateral Acceleration

The calculations will also be performed for KG from 8 to 18 m with 2 m intervals. The lower limit of 8 m is approximately the center of gravity in the ballast condition with no containers, and the upper limit of 18 m is maximum value it can acquire in any loading condition. The center of gravity affects the roll angle, the lateral acceleration and the wave slope coefficient. Only the first two are presented below:

Table 40: KG – φ and a_y

KG (m)	φ (rad)	φ (deg)	a_y (m/s²)	Status
8	0.221	12.68	3.59	**Pass**
10	0.220	12.58	3.52	**Pass**
12	0.217	12.43	3.45	**Pass**
14	0.213	12.23	3.35	**Pass**
16	0.208	11.91	3.23	**Pass**
18	0.198	11.35	3.04	**Pass**

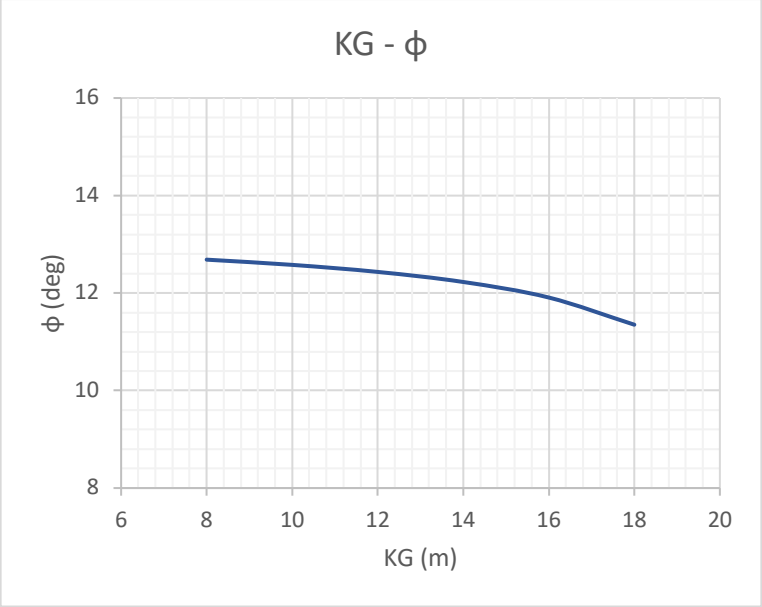

Figure 16: KG – φ

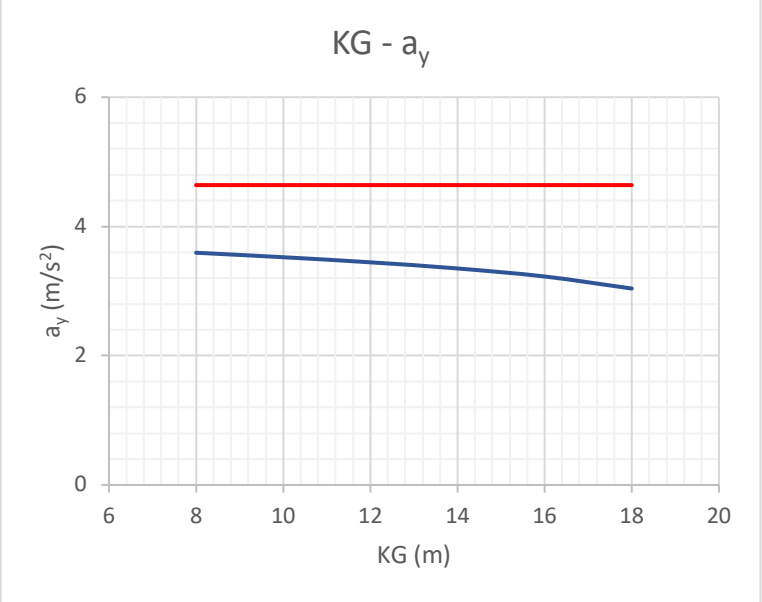

Figure 17: KG – a_y

It seems that roll angle drops slightly and the lateral acceleration remains almost constant with the increase of the center of gravity. So, the change of KG doesn't affect the final results a lot. As previously stated, higher KG results in slower ship movements and rolling angles. In the certain loading condition, the criterion cannot fail no matter the value of the KG.

5.2 Level 2 EA Criterion Results

For Level 2, all four loading conditions again, passed the criterion. There is a clear connection between Level 1 and Level 2, as higher final results in Level 1 correlate with higher results in Level 2, as well. This indicates that the two criteria are coupled with each other and that their results are interdependent, to some extent. Additionally, Tables 18, 21, 24 and 27, show the severity of every environmental condition. In every loading condition, the biggest short-term failure indices are located in the lower rows of the matrix, where the biggest waves in height are, and generally, on the left side, meaning smaller wave periods. However, their effect is mitigated, due to their unlikeness to be encountered in seas, represented by their lower weighting factor W_i. Conversely, smaller wave heights pose no danger for the ship whatsoever, as indicated by $C_{S,i}$ values of zero, in the upper portions of the Tables.

Similarly with Level 1, the effect of some particulars has to be figured out. The calculations for Level 2 will be performed as well, with the same changed parameters where Level 1 failed. Moreover, the new updated IACS scatter table will be examined. The same calculations for the four loading conditions, as in Chapter 4 will be performed. The goal is to figure out which table results in a stricter criterion and how different the two results are.

5.2.1 Different Parameters in Level 2

As previously shown, for LC36 Level 1 criterion fails at a GM around 4.3 m. Therefore, the Level 2 will be performed around this GM, until it fails, as well. This will allow to check the consistency between the two Levels and to figure out how much stricter Level 2 is compared to Level 1. Table 41 and Figure 20 present the final results for Level 2 at different GM values, with the vertical axis being logarithmic:

Table 41: Level 2 with GM values

GM (m)	Level 2	Status
4	9.17E-05	Pass
4.1	1.20E-04	Pass
4.2	1.53E-04	Pass
4.3	1.94E-04	Pass
4.4	0.000241	Pass
4.5	0.000296	Pass
4.6	0.000360	Pass
4.7	0.000433	Fail
4.8	0.000379	Fail
4.9	0.000516	Fail
5	0.000608	Fail
5.5	0.00139	Fail

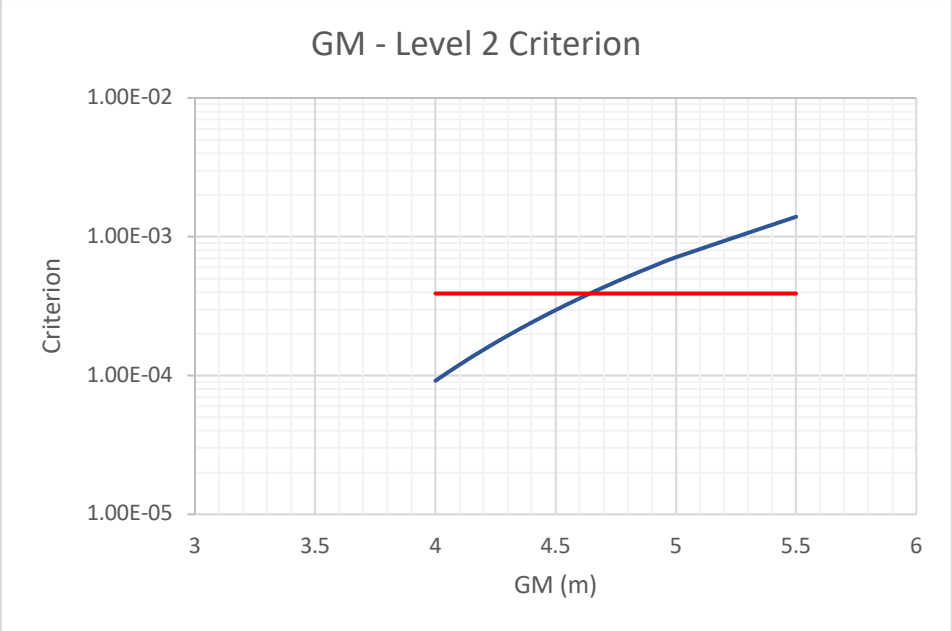

Figure 18: GM – Level 2

Firstly, the information above shows that failure of the criterion occurs at a higher GM value compared to Level 1. From Figure 20, it appears that the critical GM is slightly over 4.6 m. Therefore, an increase of around 7% in the GM value is sufficient to cause Level 2 to fail as well. This makes sense, as ships are more likely to encounter such problems in heavy weather, where the metacentric height can increase significantly, due to the action of waves. Normally, for values bigger than that, a Direct Stability Assessment (DSA) has to be conducted, to figure out what the maximum GM value is. Alternatively, DSA can be skipped, as it is considered very time consuming and the loading condition or other operational measures can be altered, to achieve stability with higher metacentric heights.

By performing the calculations for the height of the bridge deck h_k, as done for Level 1, it appears that no failure occurs for the previous critical heights. This means that no continuity errors appear in this scenario, too. Extending the calculations until failure, the critical value for the height of the bridge deck for Level 2, is around 130 m. That's about 1.5 times bigger than the critical value for Level 1, and an unreasonably high position for the bridge deck, that will never be found in vessels of such dimensions.

Similar results with Level 1, were taken for the different KG values. The center of gravity only affects slightly the Level 2 final result. Performing the calculations for the same range as Level 1 (8 to 18 m), doesn't result in failure of Level 2. The final results were in the same order of magnitude, for every scenario (10^{-8}), with the highest value appearing for the smallest KG. Therefore, lowering the center of gravity of a ship results in slightly faster rolling accelerations.

5.2.2 Different Roll Moment of Inertia in Level 2

Another parameter which is interesting to figure how it affects the criterion is the roll moment of inertia $J_{T,roll}$. The range of the calculations will be 50% to 120% of the initial $J_{T,roll}$ value. Values below 80% are probably impossible to be achieved, but were included to the calculations, to get a wider picture of their connection.

Table 42: $J_{T,roll}$ – Level 2

%$J_{T,roll}$	$J_{T,roll}$	Criterion	Status
50	5.470E+06	5.769E-03	Fail
60	6.564E+06	1.217E-03	Fail
70	7.658E+06	2.246E-04	Pass
80	8.752E+06	3.647E-05	Pass
90	9.846E+06	5.210E-06	Pass
100	1.094E+07	6.471E-07	Pass
110	1.203E+07	6.770E-08	Pass
120	1.313E+07	5.653E-09	Pass

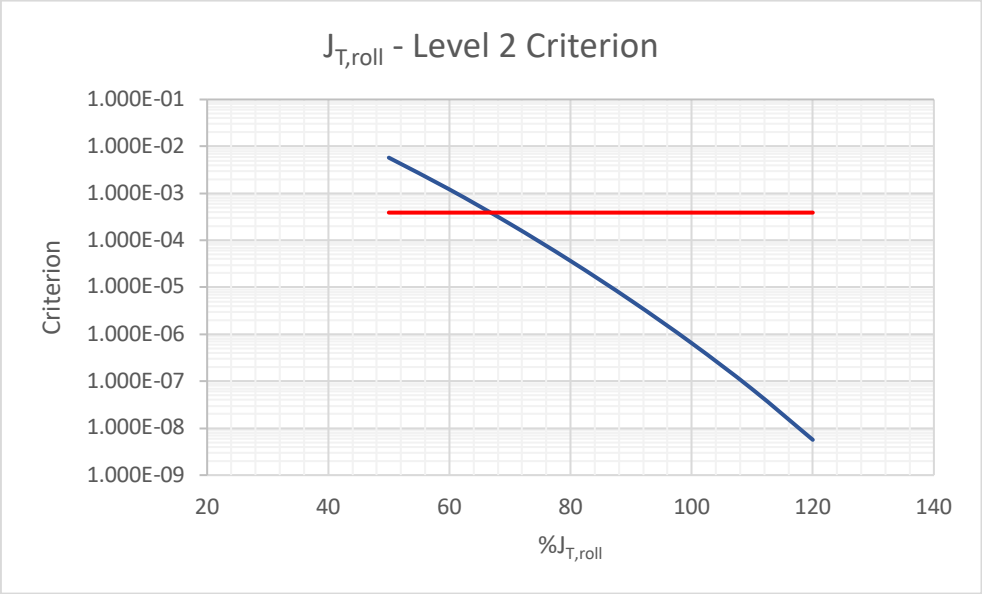

Figure 19: $J_{T,roll}$ – Level 2

It is evident that the rolling moment of inertia significantly impacts the final result of the criterion, as it was probably expected. A 10% reduction in its initial value causes the criterion to increase tenfold, indicating a very high sensitivity of this parameter. For this specific loading condition, the inertia has to be reduced by 40% for the criterion to fail. However, in a different loading condition failure can easily happen with a smaller reduction.

5.2.3 Updated IACS Table

As stated before, the IACS wave scatter table of 2001, was proposed to be updated, in 2018. Unlike the original table, Revision 2 (Rec. No. 34 rev2) is not based on human observations and estimations, but on wave modeling and data collected from Automated Identification Systems (AIS), which were installed on most ships following IMO's recommendations [26]. The new table, presented in 2023, includes different combinations of significant wave heights, H_S, and mean wave periods, T_z. Therefore, the results of the criterion will obviously be different. The question is which table, results in a stricter criterion. The Revision 2 of the table is shown in Table 43. The same calculations for the same four loading conditions as Chapter 3 are performed and the final results are shown in Table 44.

Table 43: Updated Wave Scatter Table

T_z (s) → / H_S (m) ↓	4.5	5.5	6.5	7.5	8.5	9.5	10.5	11.5	12.5	13.5	14.5	15.5	16.5	17.5	18.5	19.5
0.5	6.82	202	333.61	187.76	45.59	4.74	0.21	0	0	0	0	0	0	0	0	0
1.5	0.33	2028.35	12750.82	11693.39	7215.76	3006.8	846.07	160.77	20.63	1.79	0.1	0	0	0	0	0
2.5	0	3.38	2805.81	8517.74	7835.85	5885.37	3608.3	1805.81	737.71	246	66.96	14.88	2.7	0.4	0.05	0
3.5	0	0	23.06	2742.51	4666.81	4100.83	2936.41	1713.38	814.68	315.65	99.66	25.64	5.38	0.92	0.13	0.01
4.5	0	0	0	82.06	1759.81	2069.19	1715.42	1151.29	625.51	275.12	97.96	28.24	6.59	1.24	0.19	0.02
5.5	0	0	0	0.08	149.74	811.81	791.81	609.66	375.67	185.26	73.12	23.09	5.84	1.18	0.19	0.02
6.5	0	0	0	0	1.02	147.59	305.37	271.71	190.23	104.79	45.42	15.49	4.16	0.88	0.15	0.02
7.5	0	0	0	0	0	4.77	88.62	107.2	86.26	53.35	25.36	9.27	2.6	0.56	0.09	0.01
8.5	0	0	0	0	0	0.02	9.4	38.7	36.8	25.95	13.63	5.33	1.55	0.34	0.05	0.01
9.5	0	0	0	0	0	0	0.2	9.34	15.15	12.51	7.39	3.12	0.94	0.2	0.03	0
10.5	0	0	0	0	0	0	0	0.81	5.73	5.96	4.08	1.9	0.6	0.13	0.02	0
11.5	0	0	0	0	0	0	0	0.02	1.29	2.68	2.23	1.18	0.4	0.08	0.01	0
12.5	0	0	0	0	0	0	0	0	0.11	1.01	1.14	0.72	0.27	0.06	0.01	0
13.5	0	0	0	0	0	0	0	0	0	0.22	0.51	0.42	0.18	0.04	0	0
14.5	0	0	0	0	0	0	0	0	0	0.02	0.19	0.21	0.12	0.03	0	0
15.5	0	0	0	0	0	0	0	0	0	0	0.04	0.09	0.07	0.02	0	0
16.5	0	0	0	0	0	0	0	0	0	0	0	0.03	0.04	0.01	0	0
17.5	0	0	0	0	0	0	0	0	0	0	0	0.01	0.02	0.01	0	0
18.5	0	0	0	0	0	0	0	0	0	0	0	0	0.01	0.01	0	0

Table 44: Level 2 Results with Updated Wave Scatter Table

Loading Condition	**LC21**	**LC30**	**LC36**	**LC39**
Old Table	7.502E-9	5.947E-11	6.471E-07	1.498E-05
Updated Table	3.605E-11	7.751E-13	3.169E-09	1.032E-07
Status	**Pass**	**Pass**	**Pass**	**Pass**

Table 44 shows that the values for the final results of the updated table are approximately one hundred times smaller, in every loading condition, compared the first revision of the wave scatter table. So, the updates that were made in the table result in a less strict criterion, meaning that the initial results can be considered overly conservative.

5.3 CSM Results

First of all, looking at Table 37, no lashing force approaches the Safe Working Load (SWL). More specifically, the highest force recorded in the Table, for stack No 3 with a single lash arrangement, is only about 60% of the SWL. This shows that, generally, the lashing strength is not a major problem if the equipment is well stored and maintained. Consequently, the stowage can likely carry much heavier containers, with bigger homogenous weight, without risking the lashings breaking.

Moreover, Tables 34 – 37, indicate that the longitudinal position of the stacks affects the result only slightly. The stacks located amidship have the lowest values for transverse acceleration and lashing loads, while the stacks at the front of the ship have the highest. This can be explained, because the factor taking into account the longitudinal position on the vessel, k_3, is slightly bigger in the front of the ship. Their differences, however, are minimal and do not have any practical impact. The transverse location of the stacks plays no role in the final result, as also shown in Chapter 3. The result would be the same whether the stacks are located near the centerline or near the breadth of the ship. The top containers of the stack, being higher from the baseline, develop greater lateral acceleration, as expected. Therefore, to adequately check the criterion, performing the calculations only for the highest stack, regardless of its longitudinal and transverse location, seems sufficient.

From the two lashing arrangements, the single lash in the first arrangement and the lash No2 in the second one, develop roughly the same forces, with the single lash being slightly higher. This means that it is unclear which arrangement is better, regarding lash strength. The double lash arrangement probably offers better resistance to longitudinal movement of the stack, but this will not be studied in the current diploma thesis.

5.3.1 Comparison of CSM and EA Criterion Parameters

As previously mentioned, CSM suggests different methods for computing various parameters, needed for the application of the criterion, compared to the IMO SGISC Guidelines. The common parameters for the criteria are the natural roll period, the height of the roll axis/center, the roll angle and the lateral acceleration. For these values, CSM suggests simpler approximative formulas, depending mostly on the ship's main dimensions and its metacentric height. The results for both criteria have been mentioned before, in Chapter 4 but are presented collectively in Table 45, as well. Only the results for loading condition 36 are going to be shown:

Table 45: Comparison of IMO and CSM Parameters

Parameter	IMO symbol	CSM symbol	IMO value	CSM value
Natural Roll Period	T_r	T_r	15.05 s	17.68 s
Roll Axis/Center	h_{roll}	R_{ctr}	13.18 m	10.66 m
Roll Angle	φ	φ	12.11 °	21.95 °
Lateral Acceleration	a_y	A_T	3.30 m/s^2	5.11 m/s^2

The Table shows that all the parameters have different values with the CSM method overestimating all the results, except for the roll axis. The lateral acceleration is greater for CSM, despite being computed at a lower location in the ship. The roll amplitude is also significantly higher in the case of CSM, being nearly double. This means that the criterion's final result will also be overestimated, and if it's satisfied then the design can be considered safe.

Furthermore, looking at the final results of the two criteria, it is evident that the higher results are found in the same loading condition (LC39). Similarly, the lowest results were found in LC30 in both cases (the CSM calculations for LC30 were performed but not presented in the thesis). This indicates that the two criteria are not entirely independent and that the initial parameters affect the final result in the same way.

5.3.2 CSM Criterion with Different Metacentric Height

It is apparent that, the CSM criterion has a bigger margin until failure, compared to the EA criterion, seemingly making it the less strict one from the two. In order to further prove this point, the calculations for the CSM criterion should be performed with the same increased parameters, as before. This way, the criterion that fails first is obviously the stricter one. From the previous parameters, the height of the bridge deck, h_k, does not concern the CSM and the center of gravity, KG, and the roll moment of inertia $J_{T,roll}$ are not included in the CSM. That only leaves GM as the only common parameter. The calculations will be done for the same loading condition (LC36), for the stack located near the stem of the ship and the same GM range. The forces developed in the single lash arrangement (as it's probably the most likely to fail) will be presented in the Table below:

Table 46: GM – F_{lh1} and T_{l1}

GM (m)	F_{lh1} (kN)	T_{l1} (kN)	Status
2	67.41	98.37	Pass
3	76.48	111.61	Pass
4	85.68	125.04	Pass
5	89.50	130.60	Pass
6	93.24	136.06	Pass
7	96.94	141.46	Pass
8	100.59	146.79	Pass
9	104.21	152.08	Pass
10	107.81	157.32	Pass

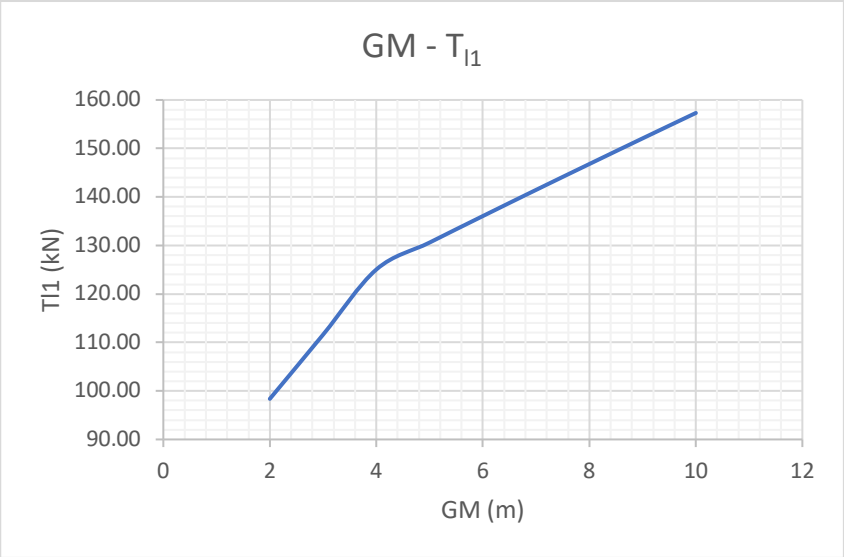

Figure 20: GM – T_{l1}

The connection between the GM and the tension of the lashings seems to be linear. The point where the incline is changed, is due to the factor C (for the computation of the roll amplitude) becoming stable and equal to 0.9 from this point forward. However, as expected, the CSM criterion proves to be the more lenient one and does not fail, even for the immense GM value of 10 m. This proves that the computation of the CSM criterion can probably be skipped, given the fact that the EA criterion is satisfied.

Chapter 6: Conclusion and Future Work

6.1 Conclusions

The analysis within this thesis explores the relevance between IMO's Excessive Acceleration Second Generation Intact Stability Criterion and the CSM calculations regarding the forces generated in container lashings. Both criteria were created to protect the lives of the crew and passengers of the ship and the integrity of its cargo, under heavy rolling movements, especially during heavy weather. The primary difference between them is that their application regards different areas on the vessel. The EA criterion focuses on locations where passenger or crew may be present and more specifically the highest place where they can be present, while the CSM criterion addresses cargo areas and mostly the upper deck where containers are stowed at. Another difference is that EA aims mostly to the protection of the passengers and the crew, while the CSM's main concern is the well-being of the cargo. The main goal of the thesis was to evaluate the criteria, compare their methods and results to each other and suggest if the application of either one can be neglected, given that the other is satisfied.

A code was developed in the Wolfram Mathematica programming language, that executes the calculations explained in the regulatory framework of the two criteria. Only Level 1 and Level 2 for the EA criterion were included in the current work. The dimensions and parameters of a model ship were inserted in the code and the calculations were conducted for four different loading conditions. The final results showed that all three criteria (the two Levels of EA and the CSM) were satisfied for all four loading conditions. Therefore, there could not be a clear comparison between them and determine which one is the stricter and which one is the more lenient. In order to make to comparison some of the parameters were altered, to figure which criterion fails first and which of the parameters influences the most the final result, and thus the safety of the ship. From all the parameters that were checked the most crucial and sensitive seemed to be the metacentric height, affecting significantly all three criteria. Also, the roll moment of inertia affected greatly the Level 2 of the EA criterion. A slight increase in the moment's value resulted in immense difference in the criterion's final result, making it one the most important factors to take into account, when studying the roll movement and the lateral acceleration of a ship.

From that analysis it was concluded that the CSM criterion is the most lenient. In all the scenarios studied, the forces of the lashings never exceeded the critical value of the Safe Working Load, indicating that the criterion was always satisfied. Level 2 EA criterion proved always stricter than Level 1, because Level 1 was always satisfied if Level 2 was satisfied, as it is supposed to be. This indicates that no continuity errors appear between the two Levels. The three criteria are clearly somewhat connected, as larger and smaller final results are found in the same loading conditions. However, as mentioned, in all the scenarios studied, when the EA criterion was met, the CSM was as well. So, it is a reasonable assumption to be made, that the CSM criterion for the lashing loads can generally be omitted, and only the EA criterion suffices for both. If the EA criterion proves to be satisfied then it seems almost certain that the CSM criterion will be met as well.

After that analysis was concluded, the Level 2 EA criterion was computed again, this time using the updated and revised IACS wave scatter table. This table was introduced in 2023, in order to replace the older one. The final results show that the new table is more lenient and the old table overestimated the final results.

6.2 Future Work

In order to extend the study work and deepen the results and findings presented previously, some suggestions for future work can be made. Firstly, more simulations for the criteria can be performed for other model ships of different type with different sizes, main dimensions and loading conditions. It's evident that the ship's size greatly impacts its stability characteristics and so it would be a good start to further inspect the strictness of the criteria. Moreover, the DSA can be performed as well and be compared with the thesis' findings. Despite being overly complicated and time consuming for DSA to be conducted, it would be important to compare its results with the respective results for Level 1 and 2 of the criterion. The modeling of the containers can be further studied and analyzed. Heavier containers with different homogenous weight and different dimensions can be examined. Also, the possibility of the container to slide or trip over, under the influence of both roll and pitch motions can be considered. Alternative lashing arrangements and securing methods can be checked as well.

Chapter 7: Bibliography

[1] Κ. Σπύρου, Μελέτη και Εξοπλισμός ΙΙ, Σημειώσεις Διδάσκοντος και Πρόσθετο Βοηθητικό Υλικό, Εθνικό Μετσόβιο Πολυτεχνείο, 2020.

[2] Κ. Σπύρου, Δυναμική Ευστάθεια Πλοίου, Εθνικό Μετσόβιο Πολυτεχνείο.

[3] A. Francescutto, "Intact stability criteria of ships– Past, present and future," *Ocean Engineering,* vol. 120, pp. 312-317, 2016.

[4] IMCO, "RECOMMENDATION ON INTACT STABILITY FOR PASSENGER AND CARGO SHIPS UNDER 100 METRES IN LENGTH," in *RESOLUTION A.167*, 1968.

[5] IMO, "ADOPTION OF THE INTERNATIONAL CODE ON INTACT STABILITY," in *RESOLUTION MSC.267(85)*, 2008.

[6] Γ. Τζαμπίρας, Υδροστατική και Ευστάθεια Πλοίου, Εθνικό Μετσόβιο Πολυτεχνείο, 2015.

[7] IMO, "RECOMMENDATION ON A SEVERE WIND AND ROLLING CRITERION (WEATHER CRITERION) FOR THE INTACT STABILITY OF PASSENGER AND CARGO SHIPS OF 24 METRES IN LENGTH AND OVER," in *RESOLUTION A.562(14)*, 1985.

[8] N. Themelis, "Probabilistic Assessment of Ship Dynamic Stability in Waves," Athens, 2008.

[9] IMO, "CODE ON INTACT STABILITY FOR ALL TYPES OF SHIPS COVERED BY IMO INSTRUMENTS," in *RESOLUTION A.749 (18)*, 1993.

[10] N. Petacco and P. Gualeni, "IMO Second Generation Intact Stability Criteria: General Overview and Focus on Operational Measures," *Journal of Marine Science and Engineering ,* 2020.

[11] IMO, "INTERIM GUIDELINES ON THE SECOND GENERATION INTACT STABILITY CRITERIA," in *SDC 7/16, Annex 5*, 2020.

[12] V. Belenky, "CONTINUED DEVELOPMENT OF SECOND GENERATION INTACT STABILITY CRITERIA," Naval Surface Warfare Center Carderock Division, West Bethesda, 2020.

[13] BSU, "Fatal accident on board the CMV CHICAGO EXPRESS during Typhoon 'HAGUPIT' on 24 September 2008 off the coast of Hong Kong," Bundsstele für Seeunfallunrschung, Hamburg, 2009.

[14] BSU, "Fatal accident on board the CMV CCNI GUAYAS during Typhoon 'KOPPU' on 15 September 2009 in the sea area off Hong Kong," Bundsstele für Seeunfallunrschung, Hamburg, 2011.

[15] IMCO, "SAFE STOWAGE AND SECURING OF CARGO UNITS AND OTHER ENTITIES IN SHIPS OTHER THAN CELLULAR CONTAINER SHIPS," in *RESOLUTION A.489(XII)*, 1981.

[16] IMO, "CONTAINERS AND CARGOES (BC) - CARGO SECURING MANUAL," in *MSC/Circ.385*, 1985.

[17] IMO, "GUIDELINES FOR THE PREPARATION OF THE CARGO SECURING MANUAL," in *MSC/Circ.745*, 1996.

[18] IMO, "CODE OF SAFE PRACTICE FOR CARGO STOWAGE AND SECURING," in *RESOLUTION A.714 (17)*, 1991.

[19] DNV, "CARGO SECURING MODEL MANUAL," 2004.

[20] V. Shigunov, "On the Consideration of Lateral Accelerations in Ship Design Rules," in *12th International Ship Stability Workshop*, Washington DC, USA, 2011.

[21] D. Paroka, A. H. Muhammad and S. Rahman, "Estimation of Effective Wave Slope Coefficient of Ships with Large Breadth and Draught Ratio," *KAPAL, Jurnal Ilmu Pengetahuan dan Teknologi Kelautan,* vol. 17, pp. 40-49, 2020.

[22] S. Rudakovic, G. Bulian and I. Backalov, "Effective wave slope coefficient of river-sea ships," *Ocean Engineering,* vol. 192, 2019.

[23] IACS, "Standard Wave Data Recommendation No.34," 2001.

[24] IMO, "DEVELOPMENT OF EXPLANATORY NOTES TO THE INTERIM GUIDELINES ON SECOND GENERATION INTACT STABILITY CRITERIA, Physical background and mathematical models for stability failures of the second generation intact stability criteria," in *SDC 8/INF.2*, 2021.

[25] CR CLASSIFICATION SOCIETY, "GUIDELINES FOR CERTIFICATION OF CONTAINER SECURING SYSTEMS," 2016.

[26] H. Austefjord, G. de Hauteclocque, T. Zhu and M. C. Johnson, "Update of wave statistics standards for classification rules," in *9th International Conference on Marine Structures*, 2023.